coexpression of IL-4 significantly skewed the Ag-specific immune response to Th2 and inhibited the induction of Graves' hyperthyroidism. In contrast, immune deviation to Th1 by coexpression of IL-12 had no effect on disease induction. Our findings reinforce the implication of the TSAb subclass data in humans, namely, that Th1-type responses mediate Graves' disease.

Materials and Methods

Adenovirus vectors used

Adenovirus expressing the human TSHR (AdCMVTSHR) has previously been described (15). Adenoviruses expressing mouse IL-12 or mouse IL-4 were constructed according to a recently described method (16, 17). The plasmid pBSKS$^-$ IL-12BIA containing cDNAs for mouse IL-12 p35 and p40 linked with the internal ribosome entry site gene of encephalomyocarditis virus (18) (kindly provided by Dr. H. Yamamoto, Osaka University, Osaka, Japan) was digested with *Eco*RV and *Not*I. The plasmid pBSKS$^+$ mIL4 containing cDNA for mouse IL-4 (RIKEN DNA Bank, Tsukuba, Japan) was digested with *Eco*RI, blunt-ended with DNA T_4 polymerase, and digested with *Not*I. These fragments were ligated into pHMCMV6 (16) which had been digested with *Nhe*I, blunt-ended, and digested with *Xba*I. The resultant plasmids pHMCMVIL-12 and pHMCMVIL-4 were then digested with I-*Ceu*I/PI-*Sce*I, and ligated into I-*Ceu*I/PI-*Sce*I-digested pAdHM15-RGD (17). pAdHMRGDCMVIL-12 and pAdHMRGDCMVIL-4 were linearized with *Pac*I and transfected into 293 human embryonal kidney cells with PolyFect (Qiagen, Tokyo, Japan) according to the manufacturer's instructions. Recombinant adenoviruses expressing IL-12 or IL-4 (designated AdRGDCMVIL-12 and AdRGDCMVIL-4) were then plaque purified. Adenovirus was propagated in 293 human embryonal kidney cells and purified through two rounds of CsCl density gradient centrifugation. The viral particle concentration was determined as previously described (15). The multiplicity of infection (MOI) was defined as the ratio of total number of particles used in a particular infection divided by the number of cells.

Immunization protocol

Female BALB/c mice (6 wk old) were purchased from Charles River Breeding Laboratory (Tokyo, Japan). All experiments were conducted in accordance with the principles and procedures outlined in the *Guidelines for the Care and Use of Laboratory Animals* at the Nagasaki University (Nagasaki, Japan). Mice were kept in a specific pathogen-free condition through the experiments. For immunization, mice were injected i.m. with 50 μl of PBS containing 10^{11} particles of AdCMVTSHR alone or in combination with 5×10^{10} particles of AdRGDCMVIL-4 or AdRGDCMVIL-12. The same immunization schedule was repeated twice at 3-wk intervals. Blood was drawn from tails before the second and third immunizations and 3 wk after the third immunization and by cardiac puncture 8 wk after the third immunization. Thyroid glands were preserved for histology.

In a therapeutic setting, AdRGDCMVIL-4 (5×10^{10} particles/mouse) alone or in combination with AdCMVTSHR (10^{11} particles/mouse) was injected twice at a 2-wk interval into mice that were in a hyperthyroid state 8 wk after three injections of AdCMVTSHR.

Thyroxine (T_4), TSAb, thyroid-stimulating hormone (TSH)-blocking Abs (TBAb), and TSH-binding inhibiting Ab (TBIAb) measurements

Total T_4 in murine sera was measured with a commercially available RIA kit (RIA-gnost tT_4; Nippon Schering, Osaka, Japan). The normal range was defined as the mean ± 3 SD of control mice.

TSAb activities in murine sera were measured with FRTL5 cells as previously described (15). The cells were seeded at 3×10^4 cells/well in a 96-well culture plate and incubated in 50 μl of hypotonic HBSS containing 0.5 mM isobutyl-methylxanthine, 20 mM HEPES, 0.25% BSA, and 5 μl of serum for 2 h at 37°C. cAMP released into the medium was measured with a cAMP RIA kit (Yamasa, Tokyo, Japan). A value over 150% of control mice was judged as positive. TBAb activities were measured in the same hypotonic buffer supplemented with 100 mU/ml bovine TSH (Sigma-Aldrich, St. Louis, MO) and were expressed as percent inhibition of TSH-induced cAMP generation by test sera.

TBIAb values were determined with a commercially available TRAb kit (BRAHMS Diagnostica, Berlin, Germany). Ten microliters of serum was used for each assay. A value over 15% inhibition of control binding was judged as positive.

ELISA for TSHR Abs

ELISA for detecting mouse IgG Abs against the TSHR was as previously reported (11, 13) with minor modifications. TSHR-289, a variant of the receptor expressed in eukaryotic cells that corresponds approximately to the extracellular A subunit (19), was affinity purified from culture medium (20). ELISA wells were coated overnight with 100 μl of TSHR-289 protein (1 μg/ml) and incubated with mouse sera (1/300 dilution). After incubation with HRP-conjugated anti-mouse IgG (diluted 3000 times, A3673; Sigma-Aldrich) or subclass-specific anti-mouse IgG1 and IgG2a (diluted 1000 and 1500 times, respectively; X56 and R19-15; BD PharMingen, San Diego, CA), color was developed using *o*-phenylenediamine and H_2O_2 as substrate and the OD read at 492 nm.

Cytokine assays

COS cells seeded at 1×10^5 cells/well in a 24-well culture plate were infected with adenovirus encoding IL-12 or IL-4 at the indicated MOIs. The next day, the cells were washed three times with PBS and the culture was continued in fresh medium for 2 days. The concentrations of IL-12 or IL-4 in culture supernatants were determined with ELISA kits (BioSource International, Camarillo, CA) according to the manufacturer's protocols. Serum levels of IL-4 and IL-12 were also measured with ELISA kits (BioSource International).

Splenocytes were cultured (triplicate aliquots) at 4×10^5 cells/well in a 96-well round-bottom plate in the presence or absence of TSHR-289 protein (5 μg/ml). Five days later, the concentrations of IFN-γ and IL-4 in the medium were determined with ELISA kits (BioSource International). Cytokine production was expressed as picograms per milliliter using standard curves of recombinant murine IL-12 and IL-4 or as a fold increase relative to cultures without TSHR Ag.

Thyroid histology

Thyroid tissues were removed and fixed with 10% Formalin in PBS. Tissues were embedded in paraffin and 5-μm thick sections were prepared and stained with H&E.

Results

To investigate the effect of coexpression of IL4 or IL-12 in our murine Graves' model (15), we constructed replication-defective recombinant adenoviruses encoding IL-4 and IL-12 (AdRGDCMVIL-4 and AdRGDCMVIL-12). These adenoviruses have a RGD sequence, the binding site for $\alpha_v\beta_3$- and $\alpha_v\beta_5$-integrin, on the HI loop of the fiber knob, thus facilitating RGD/integrin-dependent viral infection (17). Although this mutant virus retains the binding activity with its cognate receptor, it exhibits higher infectivity to a variety of cells than wild-type adenovirus (17). COS cells infected

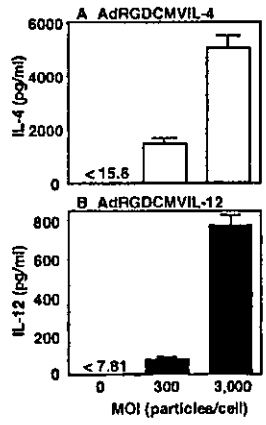

FIGURE 1. In vitro production of cytokines in COS cells infected with adenoviruses expressing either IL-4 or IL-12. The concentrations of IL-4 and IL-12 released for 2 days from COS cells infected with AdRGDCMVIL-4 or AdRGDCMVIL-12, respectively, at the MOIs indicated were measured as described in *Materials and Methods*. Data are means ± SD (n = 3) in one of two independent experiments.

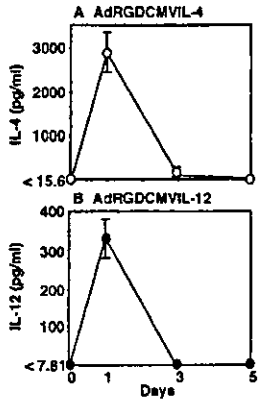

FIGURE 2. In vivo production of cytokines in mice injected with adenoviruses expressing either IL-4 or IL-12. Mice were injected i.m. with AdRGDCMVIL-4 or AdRGDCMVIL-12 (5×10^{10} particles/mouse; day 0) and bled on days 1, 3, and 5 for cytokine assays. Data are means ± SD of three mice in each group.

with AdRGDCMVIL-4 and AdRGDCMVIL-12 produced significant amounts of IL-4 and IL-12, respectively, in a MOI-dependent manner (Fig. 1). Furthermore, i.m. injection of AdRGDCMVIL-4 and AdRGDCMVIL-12 (5×10^{10} particles/mouse) to mice also increased serum concentrations of IL-4 and IL-12, respectively, although the expression was transient (Fig. 2). In vitro infection (MOI of 3000 particles/cell) or in vivo injection (10^{11} particles/mouse) of AdCMVTSHR did not induce detectable IL-4 or IL-12 (data not shown).

AdCMVTSHR alone (10^{11} particles/mouse) or in combination with AdRGDCMVIL-4 or AdRGDCMVIL-12 (5×10^{10} particles/mouse) was injected into quadriceps of female BALB/c mice three times at 3-wk intervals. As shown in Fig. 3*A*, some mice in all groups developed hyperthyroidism after the second immunization, and thereafter the incidence of hyperthyroidism increased. In our preliminary experiments, the incidence of hyperthyroidism plateaued 8 wk after the third immunization (data not shown). The serum concentration of T_4 in naive mice was 4.52 ± 0.83 μg/dl (mean ± SD). On this basis, the normal range of T_4 was defined as 2.03–7.01 μg/dl (mean ± 3 SD). Disease incidence at this time point was 60% (12 of 20) in mice immunized with AdCMVTSHR alone (TSHR group), similar to our previous study (15, 21), 53% (8 of 15) in those with AdCMVTSHR and AdRGDCMVIL-12 (TSHR plus IL-12), but only 13% (2 of 15) in those with AdCMVTSHR and AdRGDCMVIL-4 (TSHR plus IL-4) (Figs. 3*A* and 4*A*). Thus, coexpression of IL-4 significantly suppressed disease induction compared with induction by TSHR alone or by TSHR plus IL-12 ($p = 0.005$ and 0.020, respectively, χ^2 test).

By ELISA, anti-TSHR of the IgG class were detected 3 wk after the first immunization in all groups of immunized mice and the titers plateaued after the second immunization (Fig. 3*B*). TBIAb activities were detectable later, after the second immunization (Fig. 3*D*). It is at present unclear whether the TBIAb assay is less

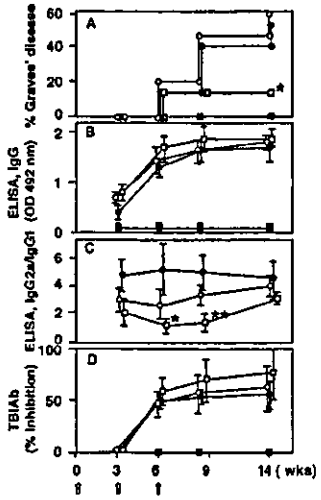

FIGURE 3. Incidence of hyperthyroidism, anti-TSHR Abs in ELISA (IgG, IgG1, and IgG2a), and TBIAb activities in mice immunized with AdCMVTSHR alone or in combination with AdRGDCMVIL-4 or AdRGDCMVIL-12. Groups of mice were immunized with AdCMVTSHR (1×10^{11} particles/mouse) alone or in combination with AdRGDCMVIL-4 or AdRGDCMVIL-12 (5×10^{10} particles/mouse) and bled for T_4 and autoantibody assays just before the second and third immunizations and 3 and 8 wk after the third immunization. *A*, Mice with T_4 more than mean ± 3 SD of control mice were judged as hyperthyroid. *, $p = 0.005$ and 0.02 for the TSHR plus IL-4 group vs the TSHR and the TSHR plus IL-12 groups, respectively (χ^2 test). *B–D*, Anti-TSHR Abs of IgG, IgG1, and IgG2a and TBIAb activities in mouse sera were measured as described in *Materials and Methods*. O, Mice immunized with AdCMVTSHR alone; ●, those with AdCMVTSHR and AdGRDCMVIL-12; □, those with AdCMVTSHR and AdRGDCMVIL-4; ■, naive mice. Data are means ± SD in *B* and *D* and means ± SE in *C*, each determined in duplicates. Arrows indicate adenovirus injections. * and **, $p = 0.021$ and 0.009 for the TSHR plus IL-4 group vs the TSHR group, respectively (Student's *t* test).

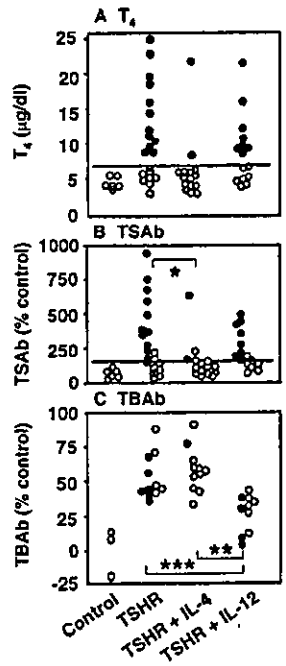

FIGURE 4. T_4 and TSAb and TBAb activities in mice immunized with AdCMVTSHR alone or in combination with AdRGDCMVIL-4 or AdRGDCMVIL-12. T_4, TSAb, and TBAb activities were determined 8 wk after the third immunization as described in *Materials and Methods*. Data are means of duplicate assays. O and ●, Euthyroid and hyperthyroid mice, respectively. TBAb activities were determined only in mice for which sufficient sera were available ($n = 10–11$ in each group). Horizontal lines indicate the normal upper limits of T_4 and TSAb assays; the normal upper limit of TBAb was not calculated because only a small number of control sera ($n = 3$) were available in this assay. *B*, *, $p = 0.036$ for the TSHR group vs the TSHR plus IL-4 group; *C*, * and **, $p = 0.0002$ and 0.001 for the TSHR plus IL-4 group vs the TSHR plus Il-4 and TSHR plus IL-12 groups, respectively (Student's *t* test).

sensitive than ELISA or whether neutral Abs (without TSAb or TBIAb activities) appear first, followed by TBIAb. In contrast to thyroid function mentioned above, there were no differences in the Ab levels measured by ELISA or TBIAb between the mice injected with the different combinations of adenovirus, namely, TSHR, TSHR plus IL-4, or TSHR plus IL-12, during the course of the experiment (Fig. 3, *B* and *D*). TSAb and TBAb activities were measured only at the end of the experiments because of limited amounts of sera. TSAb activities, positive in most hyperthyroid mice, were significantly lower in the TSHR plus IL-4 group than in the TSHR group ($p = 0.036$, Student's t test; Fig. 4*B*). TBAb activities were significantly lower in the TSHR plus IL-12 group (24.3 ± 13.1%, mean ± SD) than in the TSHR group or the TSHR plus IL-4 group (51.9 ± 14.9% and 57.9 ± 14.9%, $p = 0.0002$ and 0.0001, respectively, Student's t test; Fig. 4*C*).

Th1 vs Th2 balance was examined in two ways: 1) in terms of the IgG subclass-specific ELISA (Fig. 3*C*) and 2) cytokines secreted by splenocytes in response to TSHR Ag (Fig. 5). The IgG2a:IgG1 (Th1:Th2) ratio of anti-TSHR Abs was significantly lower in the TSHR plus IL-4 group 3 wk after the second and third immunizations as compared with TSHR and TSHR plus IL-12 groups ($p = 0.021$ and 0.009, respectively, Student's t test). However, this difference was not observed before the second immunization or 8 wk after the third immunization ($p = 0.173$ and 0.065). Although the mean IgG2a:IgG1 ratios in the TSHR/IL-12 group were slightly elevated compared with the mean values in the TSHR group throughout the experiment, the differences were not statistically significant.

Splenocytes obtained 10 days after a single injection with AdCMVTSHR secreted IFN-γ in response to TSHR Ag (Fig. 5, *A* and *B*). When expressed as fold increase, IFN-γ secretion was significantly lower in the TSHR plus IL-4 group vs the TSHR group

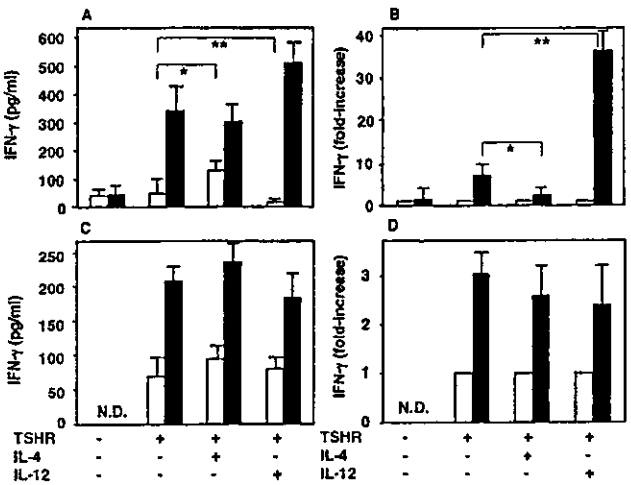

FIGURE 5. IFN-γ production from splenocytes of mice immunized with AdCMVTSHR alone or in combination with AdRGDCMVIL-4 or AdRGDCMVIL-12. Splenocytes were isolated 10 days after a single adenovirus injection (*A* and *B*) or 8 wk after three injections (*C* and *D*). IFN-γ in culture supernatants of splenocytes incubated in the presence or absence of TSHR Ag (TSHR-289, 5 μg/ml) for 5 days was determined by ELISA. Data are means ± SD ($n = 4$) and are expressed either as picograms per milliliter in *A* and *C* or as fold increase relative to cultures without TSHR-289 in *B* and *D*. □ and ■, Splenocytes cultured in the absence or presence of TSHR-289, respectively. *A*, *, $p = 0.012$ for the TSHR group vs the TSHR plus IL-4 group; **, $p = 0.027$ for the TSHR group vs the TSHR plus IL-12 group. *B*, *, $p = 0.011$ for the TSHR group vs the TSHR plus IL-4 group; **, $p = 0.0038$ for the TSHR group vs the TSHR plus IL-12 group (Student's t test). ND, Not done.

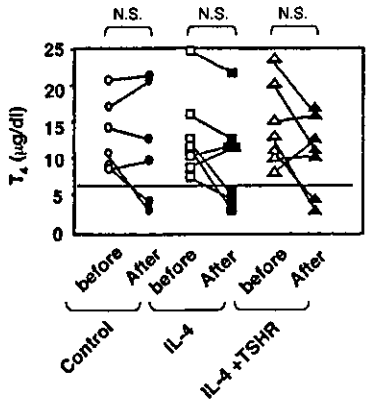

FIGURE 6. T_4 levels in hyperthyroid mice treated with AdRGDCMVIL-4 alone or in combination with AdCMVTSHR. Groups of mice (n = 6–7) that were in a hyperthyroid state 8 wk after three injections of AdCMVTSHR were treated with two i.m. injections of AdRGDCMVIL-4 (5×10^{10} particles/mouse) alone or in combination with AdCMVTSHR (10^{11} particles/mouse) at a 2-wk interval. Serum T_4 levels were measured before (■) and 2 wk after the second injection (□).

(~6-fold vs ~2.5-fold, $p = 0.011$) and significantly higher in the TSHR plus IL-12 group as compared with the TSHR group (~36-fold, $p = 0.0038$; Fig. 5*B*). However, this difference was no longer observed in splenocytes isolated from mice at the end of the experiments (Fig. 5, *C* and *D*). These data clearly demonstrate the shifting of immune response, albeit transiently, to Th1 and Th2 by IL-12 and IL-4, respectively. No IL-4 secretion was observed in mice of any group (data not shown).

Incidentally, the histology of the thyroid glands from hyperthyroid mice was essentially same among the three groups. In particular, the hyperthyroid mice had diffuse goiters with hypertrophy and hypercellularity of thyroid epithelial cells as previously reported (15), findings consistent with those in overstimulated thyroid glands. No lymphocytic infiltration was observed.

Finally, the feasibility of IL-4 for treatment of Graves' disease was evaluated. Groups of hyperthyroid mice (n = 6–7 in each group) were left untreated or injected i.m. with AdRGDCMVIL-4 (5×10^{10} particles/mouse) alone or in combination with AdCMVTSHR (10^{11} particles/mouse) twice at a 2-wk interval. Serum T_4 was measured 2 wk after the second immunization. Although the disease remitted spontaneously in some mice, the incidence of disease and mean T_4 levels were not significantly different after treatment in three groups (Fig. 6).

Discussion

We have investigated the role of IL-12 and IL-4, Th1 and Th2 cytokines, respectively, in the development of Graves' hyperthyroidism in our recently established novel murine model (15). In this model, multiple i.m. injections of TSHR-expressing adenovirus induce stimulating TSHR Abs and hyperthyroidism in >50% of female BALB/c mice. Appearance of anti-TSHR Abs of both IgG1 and IgG2a subclasses measured by ELISA and preferential secretion of IFN-γ, not IL-4, from splenocytes in response to TSHR Ag in TSHR-immunized mice reflect the induction of both Th2 and, particularly, Th1 immune responses in this model.

Coinjection of adenovirus expressing IL-4 skewed the development of the immune response against the TSHR toward the Th2 phenotype, as reflected in the decreased ratio of IgG2a:IgG1 TSHR Abs (Th1:Th2) as well as Ag-specific secretion by splenocytes of a Th1 cytokine IFN-γ. This deviation of anti-TSHR immune response away from Th1 domination was accompanied by significant suppression of stimulating TSHR Abs and hyperthyroidism.

In contrast, coinjection of adenovirus expressing IL-12 enhanced IFN-γ secretion from splenocytes, that biasing toward Th1 did not affect induction of stimulating Abs or disease incidence. It is worth noting that Ab titers determined with ELISA and TBIAb assays were not affected quantitatively by expression of either cytokine, suggesting that Ab quality, not quantity, is responsible for disease induction. Similar results have recently been observed in our adenovirus model with different mouse strains (21) as well as for DNA vaccination of outbred mice (9). The significantly lower levels of TSAb and comparable levels of TBAb in the TSHR plus IL-4 group vs the TSHR group indicate that the protective effect of IL-4 is not attributed to the increased proportion of blocking to stimulating Abs. On the other hand, the significantly lower TBAb activities in the TSHR plus IL-12 group than in the other two groups suggest that the Th1/Th2 balance influences the ratio of stimulating/blocking Abs. Overall, these data strongly indicate the crucial role of the Th1 immune response in the pathogenesis of Graves' disease in our model. Incidentally, it is unlikely that the different abilities of IgG1 and IgG2a to bind distinct FcRs and to activate complement (22) contribute to disease pathogenesis.

In this context, it is of interest that the Th2 adjuvant alum, but not the Th1 adjuvant polyriboinosinic polyribocytidylic acid, completely suppresses Ab production and disease development in another murine Graves' model we have recently established. This model involves injecting female BALB/c mice with bone marrow-derived dendritic cells infected with adenovirus expressing TSHR (23). These data suggesting the importance of Th1 immune responses in Graves' models utilizing TSHR-expressing adenovirus are consistent with our present observations, but are in sharp contrast to the previous studies with the Shimojo model of Graves' disease (10).

These apparently opposing effects of alum in different animal models, along with controversial data regarding the Th1/Th2 paradigm in experimental murine and human disease (reviewed in the Introduction), indicate that it is unwise to conclude that Graves' manifestations are the outcome of Th1-type immune responses. Moreover, the view that Th2 cytokines play a primary role in humoral autoimmune diseases may be unwarranted. Indeed, the importance of Th1 immune responses has been demonstrated in other Ab-mediated organ-specific autoimmune diseases such as autoimmune hemolytic anemia (AIHA), myasthenia gravis, and Goodpasture's disease (24). For example, preferential secretion of Th1 cytokines in response to autoantigens has been demonstrated in AIHA and myasthenia gravis (24, 25). Moreover, amelioration in AIHA was observed when mice were injected with DNA encoding IL-4 or with anti-IL-12 Ab (24). On the other hand, in murine lupus, an Ab-mediated systemic autoimmune disease (26), disease activity was suppressed in IFN-γ and IL-4 KO mice as well as in IL-4-transgenic mice (27, 28). These divergent results are not easy to reconcile and may point to the complexity of cytokine interactions.

Cytokines exert variable actions on the induction/suppression of immune response, depending on the level and location of production or the route and timing of administration. For example, IL-4, which is generally believed to stimulate humoral immunity and inhibit a Th1 immune response (29), is also shown to have the indispensable role in establishment of an early phase of Th1 immune response (30, 31). Divergent effects of certain cytokines have been reported in Th1-dominated, T cell-mediated autoimmune diseases. Thus, the therapeutic efficacy of adenovirus-mediated transiently expressed IL-4 (32) and a pathogenic role of sustained administration of rIL-4 (33) have both been demonstrated in inflammatory bowel disease. Prevention of autoimmune diabetes in nonobese diabetic mice has been achieved with systemic injection of adenovirus-expressing IL-4 (34) and also in IL-4R KO mice (35).

In conclusion, Graves' disease induced by injecting TSHR-expressing adenovirus is characterized by Th1 and to a lesser extent Th2 responses. Despite its protective effect on induction of murine Graves' disease, IL-4 had no beneficial effect in a therapeutic setting. Skewing an established immune response might be more difficult than inducing a polarized response in naive mice. Indeed, it is reported that IL-4 fails to convert an already established Th1 response into a Th2 response (36). Nevertheless, the pathogenic potential of the Th1-type immune response in Graves' hyperthyroidism suggests the need for caution in developing therapeutic strategies aimed at deviating a presumed Th2-mediated autoimmune response to Th1-dominant immunity. Furthermore, unlike murine Graves' models, Th1-dominated subclinical chronic thyroiditis likely coexists with Graves' disease in humans, as indicated by the presence of autoantibodies against thyroglobulin and thyroid peroxidase in most Graves' sera, which may also worsen with such treatment. Further studies will be required to explore the therapeutic potential of cytokine therapy in humans with Graves' disease.

Acknowledgments

We thank Dr. H. Yamamoto (Osaka University) for IL-12 p35 and p40 cDNAs and RIKEN DNA Bank (Tsukuba, Japan) for mouse IL-4 cDNA.

References

1. Rees Smith, B., S. M. McLachlan, and J. Furmaniak. 1988. Autoantibodies to the thyrotropin receptor. *Endocr. Rev. 9:106.*
2. Rapoport, B., G. D. Chazenbalk, J. C. Jaume, and S. M. McLachlan. 1998. The thyrotropin (TSH) receptor: interaction with TSH and autoantibodies. *Endocr. Rev. 19:673.*
3. Yamada, T., A. Sato, I. Komiya, T. Nishimori, Y. Ito, A. Terao, S. Eto, and Y. Tanaka. 2000. An elevation of serum immunoglobulin E provides a new aspect of hyperthyroid Graves' disease. *J. Clin. Endocrinol. Metab. 85:2775.*
4. Coles, A., M. Wing, S. Smith, F. Coraddu, S. Greer, C. Taylor, A. Weetman, G. Hale, V. K. Chatterjee, H. Waldmann, and A. Compston. 1999. Pulsed monoclonal antibody treatment and autoimmune thyroid disease in multiple sclerosis. *Lancet 354:1691.*
5. Weetman, A. P. 2002. Cytokine and autoimmune thyroid disease. *Hot. Thyroidol.*
6. Davies, T. F. 1999. The thyroid immunology of the postpartum period. *Thyroid 9:675.*
7. Weetman, A. P., M. E. Yateman, P. A. Ealey, C. M. Black, C. B. Reimer, R. C. Williams, Jr., B. Shine, and N. J. Marshall. 1990. Thyroid-stimulating antibody activity between different immunoglobulin G subclasses. *J. Clin. Invest. 86:723.*
8. Shimojo, N., Y. Kohno, K. Yamaguchi, S. Kikuoka, A. Hoshioka, H. Niimi, A. Hirai, Y. Tamura, Y. Saito, L. D. Kohn, and K. Tahara. 1996. Induction of Graves-like disease in mice by immunization with fibroblasts transfected with the thyrotropin receptor and a class II molecule. *Proc. Natl. Acad. Sci. USA 93: 11074.*
9. Costagliola, S., M.- C. Many, J.-F. Dehef, J. Pohlenz, S. Refetoff, and G. Vassart. 2000. Genetic immunization of outbred mice with thyrotropin receptor cDNA provides a model of Graves'disease. *J. Clin. Invest. 105:803.*
10. Kita, M., L. Ahmad, R. C. Marians, H. Vlase, P. Unger, P. N. Graves, and T. F. Davies. 1999. Regulation and transfer of a murine model of thyrotropin receptor antibody mediated Graves' disease. *Endocrinology 140:1392.*
11. Yan, X.- M., J. Guo, P. Pichurin, K. Tanaka, J. C. Jaume, B. Rapoport, and S. M. McLachlan. 2000. Cytokines, IgG subclasses and costimulation in a mouse model of thyroid autoimmunity induced by injection of fibroblasts co-expressing MHC class II and thyroid autoantigens. *Clin. Exp. Immunol. 122:170.*
12. Costagliola, S., P. Rodien, M.-C. Many, M. Ludgate, and G. Vassart. 1998. Genetic immunization against the human thyrotropin receptor causes thyroiditis and allows production of monoclonal antibodies recognizing the native receptor. *J. Immunol. 160:1458.*
13. Pichurin, P., X.-M. Yan, L. Farilla, J. Guo, G. D. Chazenbalk, B. Rapoport, and S. M. McLachlan. 2001. Naked TSHR receptor DNA vaccination: a Th1 T cell response in which interferon-γ production, rather than antibody, dominates the immune response in mice. *Endocrinology 142:3530.*
14. Pichurin, P., O. Pichurina, G. D. Chazenbalk, C. Paras, C.-R. Chen, B. Rapoport, and S. M. McLachlan. 2002. Immune deviation away from Th1 in interferon-γ knock-out mice does not enhance TSH receptor antibody production following naked DNA vaccination. *Endocrinology 143:1182.*
15. Nagayama, Y., M. Kita-Furuyama, T. Ando, K. Nakao, H. Mizuguchi, T. Hayakawa, K. Eguchi, and M. Niwa. 2002. A novel murine model of Graves' hyperthyroidism with intramuscular injection of adenovirus expressing the thyrotropin receptor. *J. Immunol. 168:2789.*

16. Mizuguchi, H., and M. A. Kay. 1998. Efficient construction of a recombinant adenoviral vector by an improved in vitro ligation method. *Hum. Gene Ther. 9:2577.*
17. Mizuguchi, H., N. Koizumi, T. Hosono, N. Utoguchi, Y. Watanabe, M. A. Kay, and T. Hayakawa. 2001. A simplified system for constructing recombinant adenoviral vectors containing heterologous peptides in the HI loop of their fiber knob. *Gene Ther. 8:730.*
18. Obana, S., H. Miyazawa, E. Hara, T. Tamura, H. Nariuchi, M. Takata, S. Fujimoto, and H. Yamamoto. 1995. Induction of anti-tumor immunity by mouse tumor cells transfected with mouse interleukin-12 gene. *Jpn. J. Med. Sci. Biol. 48:221.*
19. Chazenbalk, G.D., J. C. Jaume, S. M. McLachlan, and B. Rapoport. 1997. Engineering the human thyrotropin receptor ectodomain from a non-secreted form to a secreted, highly immunoreactive glycoprotein that neutralizes autoantibodies in Graves' patients' sera. *J. Biol. Chem. 272:18959.*
20. Chazenbalk, G.D., S. M. McLachlan, P. Pichurin, and B. Rapoport. 2001. A "prion-like" shift between two conformational forms of a recombinant thyrotropin receptor A subunit module: purification and stabilization using chemical chaperones of the form reactive with Graves' autoantibodies. *J. Clin. Endocrinol. Metab. 86:1287.*
21. Nagayama, Y., S. M. McLachlan, B. Rapoport, and M. Niwa. 2002. A major role for non-MHC genes, but not for microorganisms, in a novel murine model of Graves' hyperthyroidism. *Thyroid. In press.*
22. Gessner, J. E., H. Heiken, A. Tamm, and R. E. Schmit. 1998. The IgG receptor family (FcγR). *Ann. Hematol. 76:231.*
23. Kita-Furuyama, M., Y Nagayama, P. Pichurin, S. M. McLachlan, B. Rapoport, and K. Eguchi. 2002. Dendritic cells infected with adenovirus expressing the thyrotropin receptor induce Graves' hyperthyroidism in BALB/c mice. *Clin. Exp. Immunol. 131:234.*
24. Elson, C., and R. N. Baker. 2000. Helper T cells in antibody-mediated, organ-specific autoimmunity. *Curr. Opin. Immunol. 12:664.*
25. Hill, M., D. Beeson, P. Moss, L. Jacobson, A. Bond, L. Corlett, J. Newsom-Davis, A. Vincent, and N. Willcox. 1999. Early-onset myasthenia gravis: a recurring T-cell epitope in the adult-specific acethylcholine receptor ε subunit presented by the susceptibility allele *HLA-DR52a. Ann. Neurol. 45:224.*
26. Theofilopoulos, A. N., and B. R. Lawson. 1999. Tumor necrosis factor and other cytokines in murine lupus. *Ann. Rheum. Dis. 58:149.*
27. Peng, S. L., J. Moslehi, and J. Craft. 1997. Roles of interferon-γ and interleukin-4 in murine lupus. *J. Clin. Invest.* 99:1936.
28. Santiago, M.-L., L. Fossati, C. Jacquet, W. Muller, S. Izui, and L. Reininger. 1997. Interleukin-4 protects against a genetically linked lupus-like autoimmune syndrome. *J. Exp. Med. 185:65.*
29. Mossman, T. R., and R. L. Coffman. 1989. Th1 and Th2 cells: different patterns of lymphokine secretion lead to different functional properties. *Annu. Rev. Immunol. 7:145.*
30. Biedermann, T., S. Zimmermann, H. Himmelrich, A. Gumy, O. Egeter, A. K. Sakrauki, I. Seegmuller, H. Voigt, P. Launois, A. D. Levine, et al. 2001. IL-4 instructs T_H1 responses and resistance to *Leishmania major* in susceptible BALB/c mice. *Nat. Immunol. 2:1054.*
31. Rhodes, S. G., and S. Graham. 2002. Is timing important for cytokine polarization? *Trends Immunol. 23:246.*
32. Hogaboam, C. M., B. A. Vallance, A. Kumar, C. L. Addison, F. L. Graham, J. Gauldie, and S. Collins. 1997. Therapeutic effects of interleukin-4 gene transfer in experimental inflammatory bowel disease. *J. Clin. Invest. 100:2766.*
33. Fort, M., R. Lesley, N. Davidson, S. Menon, F. Brombacher, M. Leach, and D. Rennick. 2001. IL-4 exacerbates disease in a Th1 cell transfer model of colitis. *J. Immunol. 166:293.*
34. Cameron, M. J., G. A. Arreaza, L. Waldhauser, J. Gauldie, and T. L. Delovitch. 2000. Immunotherapy of spontaneous type I diabetes in nonobese diabetic mice by systemic interleukin-4 treatment employing adenovirus vector-mediated gene transfer. *Gene Ther. 7:1840.*
35. Radu, D. L., N. Noben-Trauth, J. Hu-Li, W. E. Paul, and C. A. Bona. 2000. A targeted mutation in the IL-4Rα gene protects mice against autoimmune diabetes. *Proc. Natl. Acad. Sci. USA 97:12700.*
36. Tonnetti, L., R. Spaccapedo, E. Cenci, A. Mencacci, P. Puccetti, R. L. Coffman, F. Bistoni, and L. Romani. 1995. Interleukin-4 and -10 exacerbate candidiasis in mice. *Eur. J. Immunol. 25:1559.*

Gene Therapy (2003) 10, 1891–1902

www.nature.com/gt

RESEARCH ARTICLE

Dendritic cells transduced with gp100 gene by RGD fiber-mutant adenovirus vectors are highly efficacious in generating anti-B16BL6 melanoma immunity in mice

N Okada[1], Y Masunaga[1], Y Okada[2], H Mizuguchi[3], S Iiyama[1], N Mori[1], A Sasaki[1], S Nakagawa[4], T Mayumi[4], T Hayakawa[5], T Fujita[1] and A Yamamoto[1]

[1]*Department of Biopharmaceutics, Kyoto Pharmaceutical University, Kyoto, Japan;* [2]*Department of Pharmaceutics, School of Pharmaceutical Sciences, Mukogawa Women's University, Hyogo, Japan;* [3]*Division of Cellular and Gene Therapy Products, National Institute of Health Sciences, Tokyo, Japan;* [4]*Department of Biopharmaceutics, Graduate School of Pharmaceutical Sciences, Osaka University, Osaka, Japan; and* [5]*National Institute of Health Sciences, Tokyo, Japan*

Dendritic cells (DCs) are the most potent professional antigen-presenting cells for the initiation of antigen-specific immune responses, and antigen-loaded DCs have been regarded as promising vaccines in cancer immunotherapy. We previously demonstrated that RGD fiber-mutant adenovirus vector (AdRGD) could attain highly efficient gene transduction into human and murine DCs. The aim of the present study is to demonstrate the predominance of ex vivo genetic DC manipulation using AdRGD in improving the efficacy of DC-based immunotherapy targeting gp100, a melanoma-associated antigen (MAA). Vaccination with murine bone marrow-derived DCs transduced with AdRGD encoding gp100 (AdRGD-gp100/mBM-DCs) dramatically improved resistance to B16BL6 melanoma challenge and pulmonary metastasis as compared with immunization with conventional Ad-gp100-transduced mBM-DCs. The improvement in antimelanoma effects upon immunization with AdRGD-gp100/mBM-DCs correlated with enhanced cytotoxic activities of natural killer (NK) cells and B16BL6-specific cytotoxic T lymphocytes (CTLs). Furthermore, in vivo depletion analysis demonstrated that CD8+ CTLs and NK cells were the predominant effector cells responsible for the anti-B16BL6 immunity induced by vaccination with AdRGD-gp100/mBM-DCs, and that helper function of CD4+ T cells was necessary for sufficiently eliciting effector activity. These findings clearly revealed that highly efficient MAA gene transduction to DCs by AdRGD could greatly improve the efficacy of DC-based immunotherapy against melanoma.
Gene Therapy (2003) **10**, 1891–1902. doi:10.1038/sj.gt.3302090

Keywords: *dendritic cell; adenovirus vector; fiber-mutant; gp100; melanoma; immunotherapy*

Introduction

The goal of cancer vaccines is to raise the cytotoxic immune response, in which antitumor cytotoxic T lymphocytes (CTLs) play a central role, to a level capable of tumor rejection and regression. It is well established that potent priming and subsequent activation of antitumor CTLs are required for the processing and presentation of tumor-associated antigens (TAAs) as peptide fragments in the context of appropriate major histocompatibility complex (MHC) class I molecules by antigen-presenting cells (APCs).[1] The APC system is represented by dendritic cells (DCs), which possess structural and functional capabilities that are specialized for processing and presenting antigens as peptide fragments to T cells.[2-4] Owing to their unique priming and stimulating ability to naive T cells, DCs offer new perspectives in immune intervention strategies against cancer. For this novel anticancer therapy, which is based on the activation of tumor-specific CTLs using DCs as APCs, optimal *ex vivo* TAA delivery into DCs is a key issue for attaining effective therapeutic efficacy. To date, multiple approaches have been designed for delivery of TAAs to DCs, including loading with peptides, full-length proteins, and tumor cell lysates, transfection with mRNA, fusion between DCs and tumor cells, and gene transfer via nonviral or recombinant viral vectors.[5,6] While the use of peptides still ensures antigen specificity and safety, the peptide sequence and the MHC allele presenting that peptide must be known and expressed by the individual, thereby limiting the population of patients in whom T cells can be activated. On the other hand, genetic modification of DCs with specific sequences of TAA genes offers major advantages as opposed to other approaches. Following the transduction of TAA genes into DCs, full-length TAA proteins are expected to be physiologically processed and presented via MHC class I molecules by DCs. This, therefore, is a

Correspondence: Dr N Okada, Department of Biopharmaceutics, Kyoto Pharmaceutical University, 5 Nakauchi-cho, Misasagi, Yamashina-ku, Kyoto 607-8414, Japan
Received 01 March 2003; received in revised form 20 April 2003; accepted 26 April 2003

mean for activating specific antitumor CD8+ CTLs with the full antigenic determinants spectrum. Furthermore, TAA gene-modified DCs may also present MHC class II-restricted epitope(s) to CD4+ T cells, and can express TAA continuously and MHC-peptide complexes for long periods.[7-9]

Among various techniques for transferring the TAA gene to DCs, the *ex vivo* engineering of DCs using adenovirus vector (Ad) provides encouraging results.[10-12] However, the low or lack of coxsackie–adenovirus receptor (primary Ad-receptor) expression on the DC surface makes sufficient gene transduction to DCs by conventional Ad difficult.[13-16] Likewise, the cytopathic effect of high-dose Ad on DCs remains an impediment to this strategy. We recently reported that RGD fiber-mutant Ad (AdRGD), which targets α_v-integrin during attachment to cells by insertion of the RGD peptide into the HI loop of the fiber knob,[17] exhibited highly efficient foreign gene transduction in murine and human DCs compared to conventional Ad.[15,16,18] Moreover, a murine DC line (DC2.4 cells) transduced with ovalbumin (OVA) gene by AdRGD could elicit a more effective OVA-specific immune response in vaccinated mice than a cell line transduced by conventional Ad.[18] Although these results suggest that efficient gene transduction by AdRGD would improve the efficacy of DC-based gene immunotherapy, the use of primary DCs and the targeting of natural TAA rather than a continuously proliferating DC line and highly immunogenic model antigen is desirable in order to establish the predominancy of AdRGD in DC-based immunotherapy.

Melanoma is one of the few cancers for which multiple TAAs capable of eliciting a specific cellular immune response have been identified. These include gp100, MART-1/Melan-A, tyrosinase, and tyrosinase-related protein.[19-23] Among these defined melanoma-associated antigens (MAAs), which are nonmutated self-differentiation antigens associated with melanin synthesis in normal melanocytes, gp100 appears to be a promising target antigen. Several human MHC class I-restricted peptides from gp100 have been identified, and vaccination strategies using synthetic gp100-derived peptides in conjunction with chemical adjuvant or autologous DCs have been evaluated in early phase I/II clinical trials.[24,25] The murine B16 melanoma model expresses most mouse homologs of these human MAAs, so it can be used to evaluate vaccine strategies in a preclinical setting. However, mice vaccinated with viral vectors encoding murine gp100 do not develop measurable murine gp100-specific immunity, and are apparently tolerant to murine gp100.[26,27] In contrast, immunization with human gp100-expressing viral vectors can overcome self-tolerance to gp100 in C57BL/6 mice because this approach induces human gp100-specific and also murine B16 melanoma-crossreactive T-cell responses.[26,27] Furthermore, immunization with DCs transduced *ex vivo* with human gp100 gene using conventional Ad generates more effective anti-B16 melanoma immunity than *in vivo* direct injection of human gp100-expressing Ad.[10]

In the current research, we attempted to demonstrate the predominance of AdRGD in DC-based immunotherapy using murine bone marrow-derived DCs (mBM-DCs) and targeting gp100. We found that mBM-DCs were highly susceptible to human gp100 gene transduction by AdRGD, and that *ex vivo* DC engineering with gp100 gene using AdRGD, as compared with conventional Ad, could generate more potent anti-B16BL6 melanoma immunity, as determined by protection against tumor challenge, reduction of lung metastasis, and analysis of effector activity. In addition, the efficacy of AdRGD-applied DC-based immunotherapy resulted from eliciting natural killer (NK) cells and a specific CD8+ CTLs response via a CD4+ T cell-dependent mechanism.

Results

Cytopathic effect of AdRGD-gp100- or Ad-gp100 transduction against mBM-DCs

Immature mBM-DCs from C57BL/6 mice were expanded *in vitro* for 8–14 days in the presence of granulocyte/macrophage colony-stimulating factor (GM-CSF). Flow cytometric analysis indicated that the resulting cell population was negative for B220 and CD14, and that more than 85% of these cells displayed characteristic DC surface markers, including I-A^b, CD80, CD86, and CD11c (data not shown). In order to investigate cytopathic effects of AdRGD-gp100- or Ad-gp100 transduction on mBM-DCs, we performed an MTT assay at 48 h post-transduction (Figure 1). Although cytotoxicity after transduction with each vector was not observed at a multiplicity of infection (MOI) of less than 50, the viability of AdRGD-gp100- or Ad-gp100-transduced mBM-DCs (AdRGD-gp100/mBM-DCs or Ad-gp100/mBM-DCs, respectively) tended to decrease at a MOI of 100 or more. In addition, cell damage caused by AdRGD-gp100 transduction was slightly more serious than that by Ad-gp100 transduction at a high MOI, and the viability of AdRGD-gp100/mBM-DCs fell to 80% at an MOI of 200. Flow cytometric analysis using an annexin-V and propidium iodide staining kit demonstrated that the manner of cell death under high-dose transductional conditions was partially apoptosis (data not shown). On the basis of these results, we set the MOI

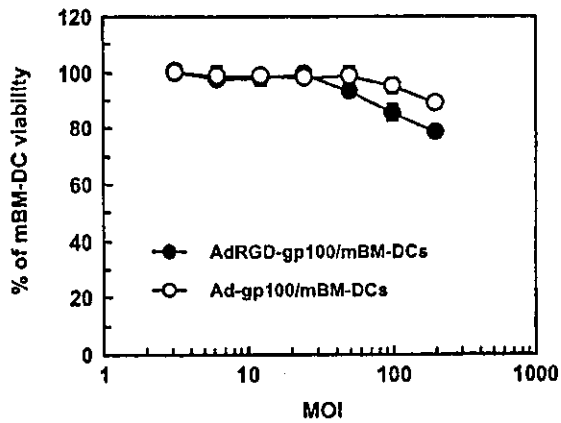

Figure 1 Cytopathic effect of AdRGD-gp100 and Ad-gp100 on gene transduction into mBM-DC. mBM-DCs were infected with AdRGD-gp100 or Ad-gp100 at the indicated MOI, and then were cultured on 96-well plates at 1 × 10^5 cells/100 μl in GM-CSF-free culture medium. After 2 days, cell viability was assessed by MTT assay. Each point represents the mean ± s.d. of triplicate cultures.

for each vector used for DC modification in the following experiments as 50 or less, which did not affect the cell viability.

Human gp100 expression in AdRGD-gp100/mBM-DCs and Ad-gp100/mBM-DCs

Expression levels of human gp100 mRNA in AdRGD-gp100/mBM-DCs and Ad-gp100/mBM-DCs were analyzed by reverse transcription-polymerase chain reaction (RT-PCR) at 48 h after transduction (Figure 2a). Human gp100-specific PCR products increased in an MOI-dependent manner in both AdRGD-gp100/mBM-DCs and Ad-gp100/mBM-DCs, whereas control vector-transduced mBM-DCs (AdRGD-LacZ/mBM-DCs) did not express any detectable gp100 mRNA. In addition, AdRGD-gp100/mBM-DCs showed much higher levels of gp100 mRNA expression than Ad-gp100/mBM-DCs. In order to confirm cytoplasmic expression of human gp100 protein, we performed flow cytometric analysis by the intracellular staining method using HMB50 antibody (Figure 2b). Under transductional conditions at an MOI of 50, more than 95% of AdRGD-gp100/mBM-DCs could express gp100 protein in their cytoplasm, whereas only 8.3% of Ad-gp100/mBM-DCs were gp100-positive. These data clearly demonstrate that AdRGD is a very potent vector system for *ex vivo* genetic modification of DCs, as we showed in our previous studies using reporter genes.[15,16,18]

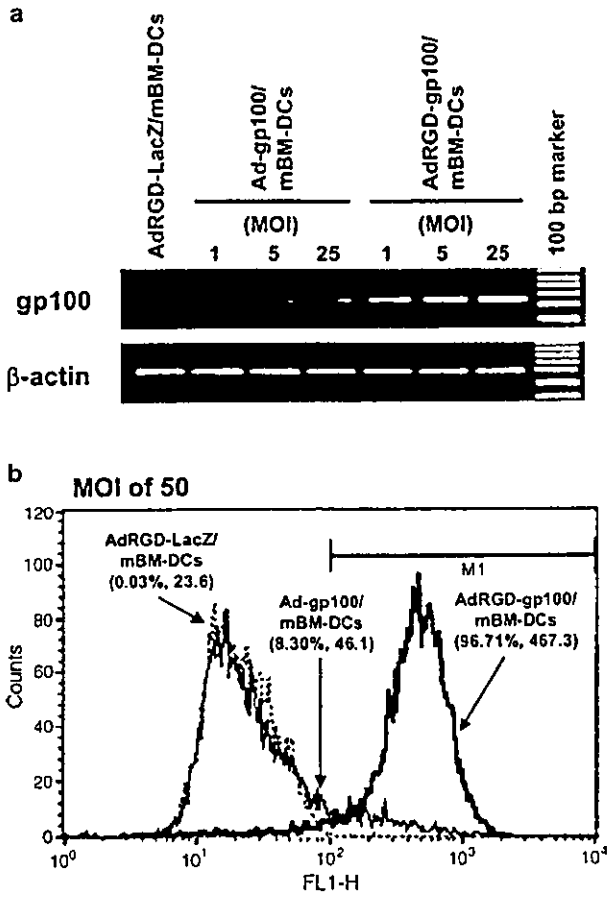

Figure 2 Human gp100 expression in AdRGD-gp100/mBM-DCs and Ad-gp100/mBM-DCs. mBM-DCs were infected with AdRGD-gp100, Ad-gp100, or AdRGD-LacZ at the indicated MOI. After 48 h cultivation, human gp100 gene expression was assessed by RT-PCR analysis (a) and flow cytometric analysis with an intracellular staining method using HMB50 antibody (b). (a) PCR for human gp100 and mouse β-actin transcripts was performed on the same RT samples using each specific primer set to ensure the quality of the procedure. (b) the % value and the numerical value in the parenthesis express % of M1-gated cells and mean fluorescence intensity, respectively.

Allogenic and syngeneic T-cell proliferation-stimulating ability of AdRGD-gp100/mBM-DCs and Ad-gp100/ mBM-DCs

Next, we performed allogenic and syngeneic mixed leukocyte reaction (MLR) to compare T-cell proliferation-stimulating ability of AdRGD-gp100/mBM-DCs and Ad-gp100/mBM-DCs. Ad-gp100/mBM-DCs could stimulate allogenic naive T cells more effectively than intact (immature) mBM-DCs, and the proliferation level of responder cells stimulated by Ad-gp100/mBM-DCs was comparable with that by lipopolysaccharide (LPS)-driving mature mBM-DCs (Figure 3a). Moreover, AdRGD-gp100/mBM-DCs could more strongly induce allogenic T-cell proliferation than Ad-gp100/mBM-DCs. On the other hand, both AdRGD-gp100/mBM-DCs and Ad-gp100/mBM-DCs, as well as intact mBM-DCs, were not able to stimulate syngeneic naive T-cell proliferation (Figure 3b). However, only AdRGD-gp100/mBM-DCs could induce the significant proliferation of syngeneic gp100-primed T cells, which were purified from C57BL/6 mouse vaccinated beforehand with 1×10^6 AdRGD-gp100/mBM-DCs, at responder/stimulator ratio of 5 (Figure 3c). These results suggested that AdRGD-gp100/mBM-DCs possessed the more potent allostimulating ability than Ad-gp100/mBM-DCs, and that they could expand syngeneic T cells in the gp100-specific manner. We determined that the T-cell proliferation-stimulating ability of AdRGD-gp100/mBM-DCs is most likely related to not only to the sufficient presentation of processed gp100 peptides via MHC molecules but also the enhancement of both costimulatory molecules expression and interleukin (IL)-12 secretion on AdRGD-gp100/mBM-DCs, which we observed previously.[16]

Vaccine efficacy of AdRGD-gp100/mBM-DCs and Ad-gp100/mBM-DCs against B16BL6 tumor challenge

C57BL/6 mice received a single intradermal injection of 1×10^6 mBM-DCs transduced with AdRGD-gp100, Ad-gp100, or AdRGD-Null at an MOI of 50, and then these mice were inoculated with 2×10^5 B16BL6 melanoma cells at 1 week postimmunization. The mice immunized with AdRGD-Null/mBM-DCs showed no significant protection against the inoculated B16BL6 cells. The results in Figure 4 demonstrated that immunization with Ad-gp100/mBM-DCs markedly inhibited B16BL6 melanoma growth when compared to the AdRGD-Null/mBM-DCs control group. In addition, a more significant inhibitory effect on tumor growth could be observed in mice after vaccination with AdRGD-gp100/mBM-DCs than in mice vaccinated with Ad-gp100/mBM-DCs. Four of six mice immunized with AdRGD-gp100/mBM-DCs

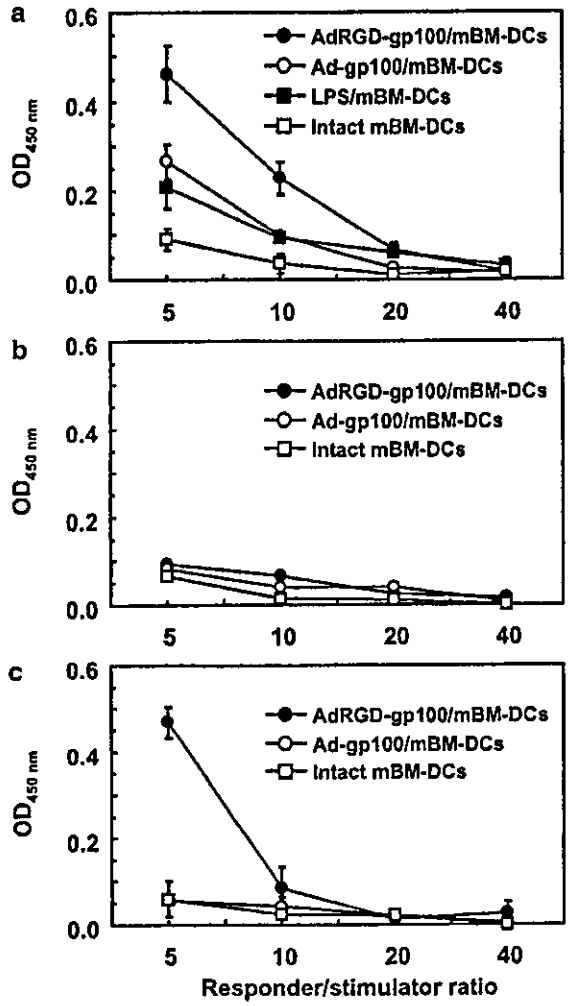

Figure 3 Allogenic and syngeneic T-cell proliferation-stimulating ability of AdRGD-gp100/mBM-DCs and Ad-gp100/mBM-DCs. C57BL/6 mBM-DCs were infected with AdRGD-gp100 or Ad-gp100 at an MOI of 50, and cultured for 2 days. Naive BALB/c T lymphocytes (a), naive C57BL/6 T lymphocytes (b), or gp100-primed C57BL/6 T lymphocytes (c) were cocultured with AdRGD-gp100/mBM-DCs, Ad-gp100/mBM-DCs, LPS/mBM-DCs, or intact mBM-DCs at different responder/stimulator ratios for 3 days. Cell cultures were pulsed with BrdU during the last 18 h, and then T-cell proliferation was assessed by BrdU-ELISA. Results are expressed as mean ± s.e. of three independent cultures using T cells prepared from thr... individual mice.

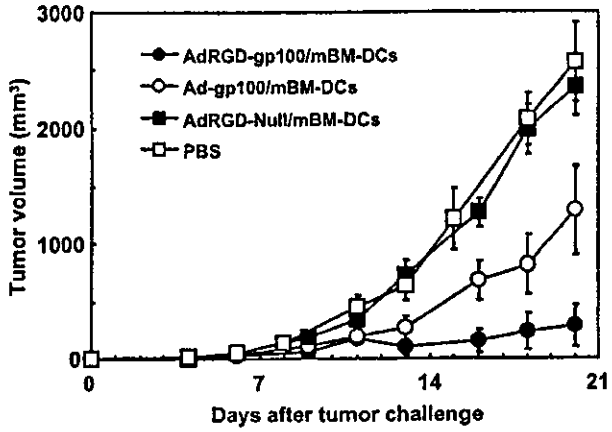

Figure 4 Vaccine efficacy of AdRGD-gp100/mBM-DCs and Ad-gp100/mBM-DCs against B16BL6 melanoma challenge. AdRGD-gp100/mBM-DCs, Ad-gp100/mBM-DCs, and AdRGD-Null/mBM-DCs were prepared using corresponding vectors at an MOI of 50. C57BL/6 mice were immunized by intradermal injection of transduced mBM-DCs into the right flank at 1×10^6 cells, and then 2×10^5 B16BL6 melanoma cells were inoculated into the mouse left flank after 1 week postvaccination. The size of tumors was assessed using microcalipers three times per week. Each point represents the mean ± s.e. from six mice.

remained tumor free for 60 days after B16BL6 cells challenge, whereas only one of six mice immunized with Ad-gp100/mBM-DCs were tumor free. Furthermore, immunization with AdRGD-gp100/mBM-DCs was specifically effective only against B16BL6 melanoma because mice vaccinated by AdRGD-gp100/mBM-DCs, as well as mice immunized with phosphate-buffered saline (PBS), did not exhibit any protective effect against syngeneic irrelevant EL4 lymphoma challenge (data not shown). These results reveal that vaccination with Ad-gp100/mBM-DCs could provide protection against B16BL6 tumor challenge, but less effectively than vaccination with AdRGD-gp100/mBM-DCs. Therefore, our data suggest that highly efficient MAA expression by application of AdRGD to *ex vivo* DC engineering could significantly enhance protective and specific antimelanoma immunity in DC-based immunotherapy.

Inhibitory effect of AdRGD-gp100/mBM-DCs and Ad-gp100/mBM-DCs on B16BL6 pulmonary metastasis

DC-based immunotherapy is expected to satisfactorily demonstrate its efficacy in prevention of metastasis and recurrence after surgical removal of the primary cancer rather than in regression of advanced primary cancer mass. Thus, we compared the anti-B16BL6 pulmonary metastasis effects of AdRGD-gp100/mBM-DCs and Ad-gp100/mBM-DCs using both the vaccine and therapeutic protocols (Figure 5). In response to the vaccine protocol, B16BL6 metastatic nodules in lung were reduced by a single immunization with AdRGD-gp100/mBM-DCs or Ad-gp100/mBM-DCs in an MOI-dependant manner, and more potent inhibitory effects were observed in the AdRGD-gp100/mBM-DCs group. The antimetastasis effect of AdRGD-gp100/mBM-DCs prepared at an MOI of 1 was comparable with that of Ad-gp100/mBM-DCs prepared at an MOI of 25, and more than 99% inhibition was attained in mice immunized with AdRGD-gp100/mBM-DCs prepared at an MOI of 25. Likewise, three immunizations with AdRGD-gp100/mBM-DCs could more effectively inhibit established pulmonary metastasis in the therapeutic protocol after intravenous injection of B16BL6 cells than Ad-gp100/mBM-DCs. These data indicate that the immunization with MAA genemodified DCs using AdRGD can greatly improve the efficacy against melanoma metastasis not only when the animals were vaccinated in advance but also when micrometastasis already existed in peripheral tissue distant from the immunization site.

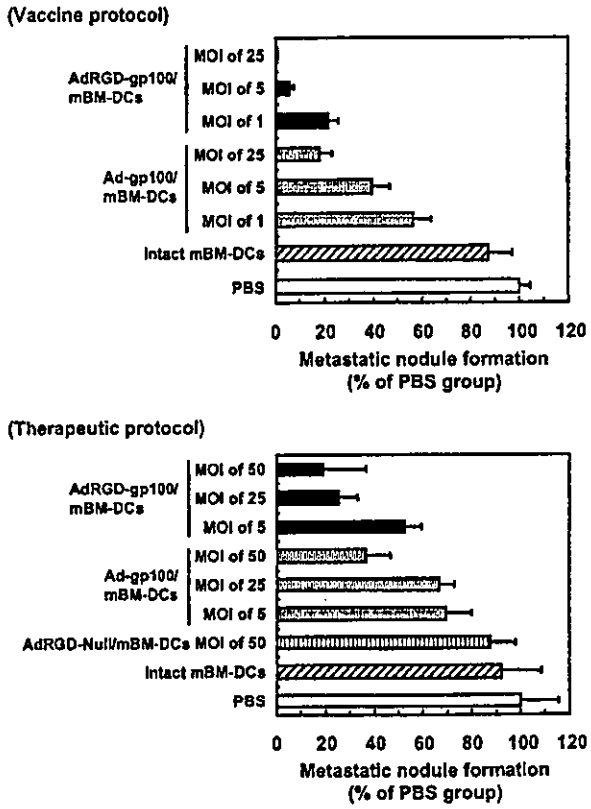

Figure 5 Inhibition of B16BL6 pulmonary metastasis by immunization with AdRGD-gp100/mBM-DCs or Ad-gp100/mBM-DCs. AdRGD-gp100/mBM-DCs, Ad-gp100/mBM-DCs, and AdRGD-Null/mBM-DCs were prepared using corresponding vectors at the indicated MOI. Experimental procedure of both vaccine and therapeutic protocols is described in the 'Materials and methods' section. Results are expressed as mean ± s.e. from six mice.

Cytolytic activity of NK cells and CTLs from mice immunized with AdRGD-gp100/mBM-DCs or Ad-gp100/mBM-DCs

In order to attain sufficient therapeutic efficacy in cancer immunotherapy, it is important to efficiently prime and activate effector cells belonging to the cellular immune system, which can directly recognize and eliminate tumor cells, rather than activate the humoral immune system. Thus, we examined the cytolytic activities of NK cells and CTLs in mice intradermally immunized with 1×10^6 AdRGD-gp100/mBM-DCs or Ad-gp100/mBM-DCs by Eu-release assay. At 1 week after immunization of C57BL/6 mice with various vaccines, the splenocytes were used in a cytolytic assay against YAC-1 cells, and were restimulated *in vitro* with inactivated B16BL6 cells, which were treated with interferon (IFN)-γ to promote the expression of their MHC class I molecules, for CTL expansion.

As shown in Figure 6, the splenic NK activity increased after immunization with AdRGD-gp100/mBM-DCs, while effector cells from mice immunized with Ad-gp100/mBM-DCs exhibited equivalent NK activity to those from mice immunized with intact mBM-DCs or PBS. These data suggested that the enhancement of nonspecific immunity might be involved

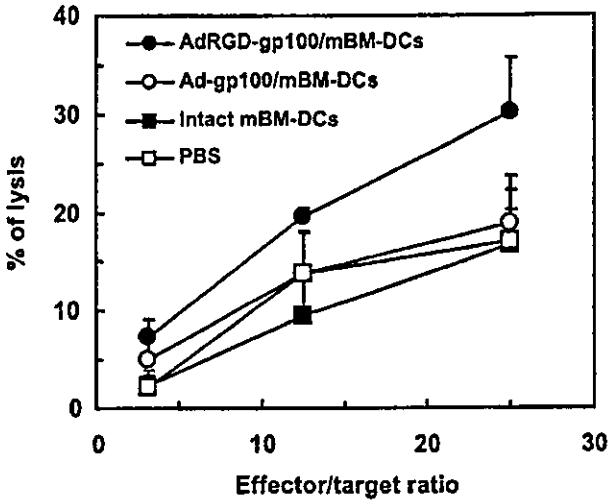

Figure 6 NK activity of splenocytes from mice immunized with AdRGD-gp100/mBM-DCs or Ad-gp100/mBM-DCs. AdRGD-gp100/mBM-DCs and Ad-gp100/mBM-DCs were prepared using corresponding vectors at an MOI of 50. Transduced or intact mBM-DCs were vaccinated once intradermally into C57BL/6 mice at 1×10^6 cells. At 1 week after immunization, nonadherent splenocytes were prepared from these mice, and directly used in cytolytic assays against YAC-1 cells. Each point represents the mean ± s.e. from three independent cultures using splenocytes prepared from three individual mice.

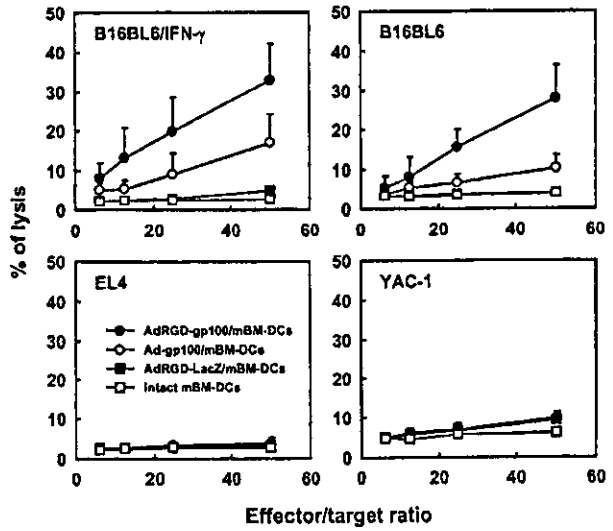

Figure 7 B16BL6-specific CTL response in mice immunized with AdRGD-gp100/mBM-DCs or Ad-gp100/mBM-DCs. AdRGD-gp100/mBM-DCs, Ad-gp100/mBM-DCs, and AdRGD-LacZ/mBM-DCs were prepared using corresponding vectors at an MOI of 50. Transduced or intact mBM-DCs were vaccinated once intradermally into C57BL/6 mice at 1×10^6 cells. At 1 week after immunization, nonadherent splenocytes were prepared from these mice, and then were restimulated in vitro for 5 days with IFN-γ-stimulated and mitomycin C-inactivated B16BL6 cells. A cytolytic assay was performed using B16BL6 cells stimulated with or without IFN-γ, EL4 cells, and YAC-1 cells. Each point represents the mean ± s.e. of three independent cultures using restimulated splenocytes prepared from three individual mice.

in the improvement of anti-B16BL6 melanoma response by AdRGD-gp100/mBM-DCs immunization. On the other hand, the cytolytic effects on B16BL6 cells by

in vitro restimulated effector cells were promoted in mice immunized with Ad-gp100/mBM-DCs as compared with mice immunized with intact mBM-DCs. However, the AdRGD-gp100/mBM-DCs group exhibited the most effective cytolytic activity (Figure 7). When B16BL6 cells stimulated with IFN-γ were used as target cells, the cytolytic activities in the groups immunized with AdRGD-gp100/mBM-DCs or Ad-gp100/mBM-DCs were still more obvious than those in the other groups. This cytolytic activity was caused by B16BL6-specific CTLs because the effector cells prepared from mice immunized with AdRGD-LacZ/mBM-DCs did not injure the B16BL6 cells and no cytolytic effects against syngeneic EL4 cells and NK-sensitive YAC-1 cells were detected in any group. Therefore, consistent with the protective and therapeutic effect against B16BL6 tumor growth and metastasis, the mice immunized with AdRGD-gp100/mBM-DCs exhibited a B16BL6 melanoma-specific CTL response, which was more potent than that induced by immunization with Ad-gp100/mBM-DCs.

Taken together, these results suggest that immunization with MAA gene-modified DCs using AdRGD, as compared with those using conventional Ad, could more efficiently prime and activate effector cells, nonspecific NK cells, and MAA-specific CTLs, which is subsequently related to rejection and regression of melanoma.

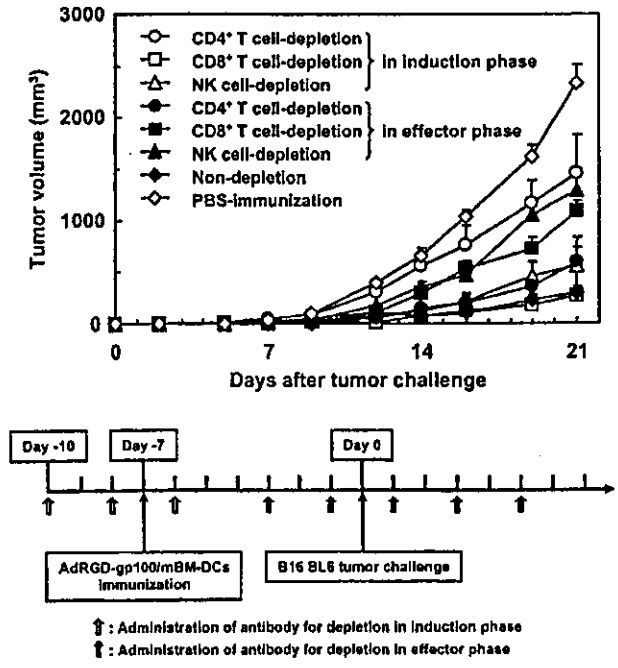

Figure 8 Determination of immune subsets responsible for the protective immunity induced by vaccination with AdRGD-gp100/mBM-DCs. C57BL/6 mice were immunized once with 1×10^6 mBM-DCs transduced with AdRGD-gp100 at an MOI of 50, and inoculated with 1×10^5 B16BL6 cells at 1 week after immunization. Antibodies, GK1.5 (anti-CD4), 53-6.72 (anti-CD8), or anti-asialoGM1, were intraperitoneally injected according to the indicated schedule. Depletion of T-cell subsets and NK cells was monitored by flow cytometry, which showed >90% specific depletion in splenocytes at the time of immunization or tumor challenge in each administration schedule. Each point represents the mean ± s.e. of six mice.

Effect of T-cell subsets- or NK cell-depletion on vaccine efficacy of AdRGD-gp100/mBM-DCs

In order to investigate what subset of immunocompetent cells was involved in the induction and effector phases and improve vaccine efficacy by immunization with AdRGD-gp100/mBM-DCs, we performed *in vivo* depletion analysis using specific antibodies against CD4, CD8, and asialoGM1. The antibody administration schedule for this experiment is shown in the lower part of Figure 8. Upon depletion during immunization (induction phase), intraperitoneal administration of each antibody was started 3 days before AdRGD-gp100/mBM-DCs immunization. These mice then received two administrations every other day. Flow cytometry showed >90% specific depletion in splenocytes from these mice at immunization, and the number of specific cells recovered was at least 70% at the time of B16BL6 tumor challenge (data not shown). On the other hand, to deplete specific cell types during tumor challenge (effector phase), antibody administration was started 3 days before B16BL6 tumor challenge. This was followed by four additional administrations performed every other day. These mice showed >90% specific depletion in splenocytes at tumor challenge, and 50–70% recovery of specific cells was observed on day 12 post-tumor challenge (data not shown).

As shown in Figure 8, the depletion of $CD8^+$ T cells or NK cells during the effector phase abrogated the protective immunity induced by immunization with AdRGD-gp100/mBM-DCs, whereas mice whose $CD4^+$ T cells were depleted during the effector phase could resist B16BL6 tumor challenge as well as nondepletion group. In contrast, mice depleted of $CD4^+$ T cells during the induction phase failed to reject B16BL6 tumor challenge. However, the depletion of $CD8^+$ T cells or NK cells during the induction phase did not influence vaccine efficacy of AdRGD-gp100/mBM-DCs. These results confirmed that $CD8^+$ CTLs and NK cells were predominant effector cells in anti-B16BL6 melanoma immunity induced by immunization with AdRGD-gp100/mBM-DCs, and that the activation of effector cells was greatly dependent on the helper function of $CD4^+$ T cells activated during the induction phase.

Discussion

In general, DCs capture antigens in the periphery and then migrate to T-cell areas in lymphoid organs to prime the antigen-specific immune responses.[4,28] Owing to these features and establishment of methods for expansion of human and rodent DCs on a large scale from hematopoietic precursors in the presence of appropriate cytokine cocktails,[29-31] DCs have attracted great attention as vehicles for the delivery of cancer vaccines. The efficacy of different viral vectors, including retroviral vector,[8,32] Ad,[8-12] and lentiviral vector,[33,34] has been evaluated for genetic modification of DCs. Among them, Ad was confirmed as a good candidate because of its high efficiency and minimum risk associated with insertional mutagenesis.[35] Owing to the life span and migration period of DCs administered to a living body,[36,37] the indication that only transient gene expression can be attained by Ad-mediated gene transfer will not impact DC-based immunotherapy. Genetic DC

modification using Ad to express TAA has been actually documented to be efficacious to induce antitumor immunity in animal models.[10-12] Nevertheless, the antitumor immunity induced by TAA gene-modified DC vaccine is still limited in clinical trials,[38,39] suggesting that the breakthrough capable of improving the efficacy of DC-based immunotherapy will need to be explored for wide application of this novel cancer treatment. The antitumor efficacy of immunization with DCs genetically modified with TAA gene is still far from satisfactory in translational research and early phase clinical trials for a variety of reasons and is partly due to the relative resistance of DCs against gene transduction. From the perspective of the exploitation of DC-based immunotherapy, we previously reported a method using AdRGD that enhances the *ex vivo* gene transduction efficiency of murine and human DCs.[15,16,18]

In recent years, the cloning of various MAAs interacting with the melanocyte differentiation and melanogenesis pathways has opened new possibilities for the development of active immunotherapy designed to cause the rejection of malignant melanoma.[19-23] gp100, an MAA, is consistently expressed in both murine and human melanomas,[27,40] and has been shown to be highly immunogenic and an important target for active-specific immunotherapy in humans.[41] However, mice injected with Ad[26] or recombinant vaccinia virus[27] encoding murine gp100, which was cloned from a B16 cDNA library, failed to produce any detectable T-cell responses or protective immunity against murine B16 melanoma. In contrast, immunization of mice with human gp100 gene, which shares 75.5% nucleotide and 77% amino-acid identity to murine gp100, using Ad elicited T cells specific for human gp100. However, these T cells also crossreacted with B16 tumor *in vitro* and could induce some level of protective tumor immunity in C57BL/6 mice against B16 challenge.[26,27] Hence, the primary aim of the present study was to demonstrate that the highly efficient transduction of mBM-DCs with a natural MAA, human gp100 gene, by AdRGD can improve the therapeutic efficacy of DC-based vaccine in the mouse B16BL6 melanoma model.

When the cytopathic effect of AdRGD-gp100- or Ad-gp100 transduction on mBM-DCs was evaluated at first, neither vector type affected cell viability at the lower MOI of 50. Although AdRGD-gp100 damaged mBM-DCs more than Ad-gp100 at an MOI of 100 or more, this phenomenon resulted from the presence of more AdRGD-gp100 particles capable of infecting and invading mBM-DCs than Ad-gp100 particles. In fact, expression of both gp100 mRNA and gp100 protein was notably higher under noncytotoxic transductional conditions in AdRGD-gp100/mBM-DCs than in Ad-gp100/mBM-DCs. Surprisingly, nearly all AdRGD-gp100/mBM-DCs could express gp100 protein in their cytoplasm under transductional conditions at an MOI of 50, and the percentage of gp100-positive cells between AdRGD-gp100/mBM-DCs and Ad-gp100/mBM-DCs resulted in a 10-fold difference. Although data were not shown, we confirmed that AdRGD was able to transduce the reporter gene into mBM-DCs more efficiently under the same transductional conditions, based on MOI or on the number of vector particles, than type 35 fiber-modified Ad whose high gene transduction efficiency in human DCs was reported by Rea *et al*.[42] Therefore, we are fully confident that AdRGD has the highest capability to genetically modify DCs *ex vivo* among the various vector systems established to date. Furthermore, AdRGD-gp100/mBM-DCs could stimulate allogenic naive T cells more effectively than Ad-gp100/mBM-DCs and also mature LPS/mBM-DCs, and the proliferation of syngeneic gp100-primed T cells was observed only in cocultivation with AdRGD-gp100/mBM-DCs. We previously demonstrated that antigen presentation level via MHC molecules in mBM-DCs transduced with the OVA gene by AdRGD was much greater than that in mBM-DCs transduced with conventional Ad.[16] Likewise, we found that AdRGD transduction could enhance the expression of MHC and costimulatory molecules and the secretion of IL-12 in mBM-DCs as compared with conventional Ad transduction.[16] Thus, we expected that AdRGD-gp100/mBM-DCs could stimulate more repertories of T-cell receptors via gp100 peptides–MHC complexes than Ad-gp100/mBM-DCs and LPS/mBM-DCs because they may sufficiently present peptides produced by processing of gp100 proteins that are expressed in large quantities within the cytoplasm. Also, they could provide secondary signals for activation and proliferation of naive T cells via costimulatory molecules whose expression levels were promoted by AdRGD transduction. In addition, IL-12 secreted from mature AdRGD-gp100/mBM-DCs might participate in potent T-cell stimulation because IL-12 is a major Th1-driving cytokine.

As expected, a single vaccination with AdRGD-gp100/mBM-DCs could provide C57BL/6 mice with much higher resistance against tumor growth and lung metastasis from subsequent B16BL6 challenge than Ad-gp100/mBM-DCs. Moreover, in the therapeutic protocol that called for three DC immunizations after intravenous injection of B16BL6 cells, mice immunized with AdRGD-gp100/mBM-DCs could more largely reduce the number of metastatic nodules than those in the Ad-gp100/mBM-DCs group. The difference between AdRGD-gp100/mBM-DCs and Ad-gp100/mBM-DCs in vaccine and therapeutic efficacy against B16BL6 melanoma reflected the gene transduction efficiency and the maturation status to mBM-DCs by AdRGD-gp100 and Ad-gp100. As the prognosis of patients with melanoma is generally poor even after surgery, chemotherapy, or radiotherapy, and the melanomas commonly metastasize,[43,44] the fact that immunization with AdRGD-gp100/mBM-DCs could demonstrate more potent therapeutic efficacy against pre-existing B16BL6 metastasis is significant. Taken together, our results indicate that highly efficient MAA gene transduction to DCs using AdRGD leads directly to the generation of very effective APCs and an improvement in the efficacy of DC-based immunotherapy against melanoma.

As DCs are uniquely capable of presenting novel antigens to naive T cells, previous studies of immune responses after immunization using antigen-loaded DCs have focused on generating antigen-specific CTLs. However, several recent reports confirm that DCs can activate NK cells and play an important role in crosstalk between innate and acquired immune responses.[45,46] We, therefore, attempted to analyze the mechanism behind the anti-B16BL6 tumor effects of immunization with AdRGD-gp100/mBM-DCs. Splenocytes from mice immunized with AdRGD-gp100/mBM-DCs could injure

YAC-1 cells more effectively than those from intact mice, whereas NK activity did not change upon immunization with Ad-gp100/mBM-DCs or intact mBM-DCs. Although data were not shown, we confirmed that the increase in NK activity in mice immunized with AdRGD-gp100/mBM-DCs disappeared 2 weeks postimmunization. We speculated that the increase in NK activity during the early stage of immunization with AdRGD-gp100/mBM-DCs was caused by upregulation of IL-12 secretion from mBM-DCs transduced with AdRGD as observed in our previous work.[16] Recently, Miller *et al*[47] also suggested that the enhancement in NK activity in mice immunized with Ad-transduced DCs depended partially on IL-12 levels secreted from immunized DCs. On the other hand, the increase in B16BL6-specific CTL activity was detected in mice immunized with Ad-gp100/mBM-DCs, and more effective cytolytic activity against B16BL6 cells was observed in effector cells prepared from mice immunized with AdRGD-gp100/mBM-DCs. These data revealed that highly efficient transduction of MAA genes to DCs using AdRGD could elicit both NK activity and melanoma-specific CTL activity more effectively than the use of conventional Ad in DC-based immunotherapy. Furthermore, the depletion of $CD4^+$ T cells during the induction phase greatly reduced the inhibition of B16BL6 tumor growth, whereas vaccine efficacy of AdRGD-gp100/mBM-DCs was not affected by $CD8^+$ T cell- or NK cell depletion during the induction phase. These data provided three important observations related to anti-B16BL6 tumor immunity generated by the immunization with AdRGD-gp100/mBM-DCs: (1) sufficient activation of the effector cells capable of demonstrating excellent anti-B16BL6 tumor effects was greatly dependent on $CD4^+$ T cells activated beforehand by administered AdRGD-gp100/mBM-DCs; (2) despite endogenous antigen presentation by gene transfer, AdRGD-gp100/mBM-DCs might present not only MHC class I-restricted epitope(s) but unidentified class II-restricted epitope(s) that are recognized by $CD4^+$ T cells; (3) the period when AdRGD-gp100/mBM-DCs could prime and activate $CD4^+$ T cells after immunization was relatively short because we confirmed that the number of $CD4^+$ T cells recovered to more than 70% on day 7 postimmunization in $CD4^+$ T-cell-depleted mice during the induction phase. Wan *et al*[48] argued that in addition to acting as helpers during the induction phase, $CD4^+$ T cells are major effector cells in anti-B16 tumor immunity induced by immunization with DCs transduced with human gp100 using conventional Ad. However, $CD4^+$ T-cell depletion during the effector phase did not impact the protective effect against B16BL6 tumor growth in mice vaccinated with AdRGD-gp100/mBM-DCs, whereas vaccine efficacy of AdRGD-gp100/mBM-DCs was clearly weakened by $CD8^+$ T-cell or NK cell depletion during the effector phase. Therefore, in our model experiment, it was confirmed that the effector cells responsible for anti-B16BL6 tumor immunity were activated nonspecific NK cells and gp100-specific $CD8^+$ CTLs.

In conclusion, our findings demonstrate that AdRGD is a very powerful vector system that improves the efficacy of DC-based immunotherapy using primary DCs and targeting natural TAA. Genetic manipulation of DCs using AdRGD not only potentiated the efficiency of TAA gene expression, but also could increase T-cell stimulation by DCs to a greater extent than conventional Ad. As a result, a more powerful anti-B16BL6 tumor effect based on efficient activation of NK cells and $CD8^+$ CTLs, which depends on the helper function of $CD4^+$ T cells, was demonstrated in mice immunized with AdRGD-gp100/mBM-DCs. Several recent reports indicated that genetically modified DCs that express cytokine or CD40 ligand could induce effective antitumor immunity in mouse model.[49-51] If the AdRGD system is applied in these strategies, not only more potent efficacy can be attained due to highly efficient gene transduction into DCs, but the immunologic properties of the modified DCs can be analyzed in detail without sorting and collection of transduced live cells. Thus, AdRGD contributes to a significant advance in the exploitation of *ex vivo* DC manipulation for experimentally and clinically relevant vaccines.

Materials and methods

Cell lines and mice

Poorly immunogenic and highly metastatic B16BL6 melanoma cell line derived from C57BL/6 mice ($H\text{-}2^b$) was cultured in minimum essential medium supplemented with 7.5% fetal bovine serum (FBS) and antibiotics. EL4 cells, a T-lymphoma cell line of C57BL/6 origin, and YAC-1 cells, a lymphoma cell line highly sensitive to NK cells, were maintained in RPMI 1640 medium supplemented with 10% FBS, 50 μM 2-mercaptoethanol, and antibiotics. The helper cell line, 293 cells, was grown in Dulbecco's modified Eagle's medium supplemented with 10% FBS and antibiotics. Female C57BL/6 mice and female BALB/c mice ($H\text{-}2^d$), aged 7–8 weeks, were purchased from SLC Inc. (Hamamatsu, Japan). Female ICR-nu/nu mice, aged 7 weeks, were purchased from Charles River Japan, Inc. (Yokohama, Japan). All mice were held under specific pathogen-free conditions and the experimental procedures were in accordance with the Osaka University guidelines for the welfare of animals in experimental neoplasia.

Generation of mBM-DCs

Isolation and cultivation of mBM-DCs were performed according to the method of Lutz *et al*[29] and slightly modified. Briefly, bone marrow cells flushed from the femurs and tibias of C57BL/6 mice were seeded at 5×10^6 cells per sterile 100-mm bacterial grade culture dish in 10 ml of RPMI 1640 containing 10% FBS, 40 ng/ml recombinant murine GM-CSF (PeproTech EC LTD., London, England), 50 μM 2-mercaptoethanol, and antibiotics. On day 3, another 10 ml of the culture medium was added to the dish for medium replenishment. Then, every 3 days, 10 ml of the culture supernatant was collected and centrifuged at 1500 rpm for 5 min at room temperature, and the pellet was resuspended in 10 ml of fresh culture medium, and then returned to the original dish to conserve unattached cells. mBM-DCs (nonadherent cells), 8–14 days old, were harvested and used as intact immature mBM-DCs in subsequent experiments. mBM-DCs cultured for more than 24 h in media containing 1 μg/ml LPS (Nacalai Tesque, Inc., Kyoto, Japan) were used as positive controls for phenotypical DC maturation.

Preparation of recombinant Ad

The replication-deficient AdRGD-gp100 and conventional Ad-gp100, which carried human gp100 cDNA derived from pAx1-CA h-gp100 (kindly provided by Dr Hirofumi Hamada, Sapporo Medical University, Sapporo, Japan) under the control of chicken β-actin promoter, were based on early regions 1- and 3-deleted adenovirus serotype 5, and were constructed by an improved *in vitro* ligation method as described.[52-54] AdRGD-LacZ and AdRGD-Null, which were constructed previously,[15,16,18] were used as control vectors in the present study. All recombinant viruses were propagated in 293 cells, purified by two rounds of CsCl density centrifugation, dialyzed, and stored at −80°C. Titers (tissue culture infectious $dose_{50}$; $TCID_{50}$) of infective Ad particles were evaluated by end-point dilution method using 293 cells.

Viral transduction into mBM-DCs

mBM-DCs were suspended at a concentration of 5×10^6 cells/ml in FBS-free RPMI 1640 and placed in a 15-ml conical tube. Each AdRGD or Ad was added at various MOI ($TCID_{50}$/cell), the suspension was mixed well, and the tube was incubated at 37°C for 2 h with occasional gentle agitation. The cells were washed three times with PBS and resuspended in a suitable solution.

Evaluation of viability of transduced mBM-DCs

AdRGD-gp100/mBM-DCs, Ad-gp100/mBM-DCs, and intact mBM-DCs were cultured on 96-well plates at 1×10^5 cells/100 μl in GM-CSF-free culture medium. After 48 h cultivation, cell viability was assessed by MTT assay and calculated by the following formula: (% of mBM-DC viability)=(MTT activity of transduced cells)/(MTT activity of intact cells) × 100.

Analysis of gene expression levels of human gp100

AdRGD-gp100/mBM-DCs, Ad-gp100/mBM-DCs, and AdRGD-LacZ/mBM-DCs were cultured on 100-mm bacterial grade culture dishes in GM-CSF-free culture medium. After 2 days, human gp100 gene expression was assessed by RT-PCR analysis and flow cytometric analysis. RT-PCR analysis for human gp100 was performed as follows. Total RNA was isolated from transduced mBM-DCs using Sepasol-RNA I Super (Nacalai Tesque, Inc.) according to the manufacturer's instructions, and then RT proceeded for 60 min at 42°C in a 50 μl reaction mixture containing 5 μg total RNA treated with DNase I, 10 μl 5 × RT buffer, 5 mM $MgCl_2$, 1 mM dNTP mix, 1 μM random hexamers, 1 μM oligo(dT), and 100 U ReverTra Ace (TOYOBO Co., LTD., Osaka, Japan). PCR amplification of the human gp100 and mouse β-actin transcripts was performed in 50 μl of a reaction mixture containing 1 μl of RT-material, 5 μl 10 × PCR buffer, 1.25 U *Taq* DNA polymerase (TOYOBO Co., LTD.), 1.5 mM $MgCl_2$, 0.2 mM dNTP, and 0.4 μM primers. The sequences of the specific primers were as follows; human gp100: forward, 5′-tgg aac agg cag ctg tat cc-3′; reverse, 5′-cct aga act tgc cag tat tgg c-3′; mouse β-actin: forward, 5′-tgt gat ggt ggg aat ggg tca g-3′; reverse, 5′-ttt gat gtc acg cac gat ttc c-3′. After denaturation for 2 min at 94°C, 20 cycles of denaturation for 60 s at 94°C, annealing for 60 s at 58°C (human gp100) or 60°C (mouse β-actin), and extension for 60 s at 72°C were repeated and followed by completion for 4 min at 72°C. The PCR product was electrophoresed on a 3% agarose gel, stained with ethidium bromide, and visualized under ultraviolet radiation. EZ Load (BIO-RAD, Tokyo, Japan) was used as a 100 bp molecular ruler. The expected PCR product sizes were 362 bp (human gp100) and 514 bp (mouse β-actin). An intracellular staining method was used for the detection of human gp100 protein in transduced mBM-DCs. Cells (1×10^6) were fixed by incubation for 10 min in 2% paraformaldehyde, and then cell membranes were permeabilized by incubation for 5 min in 1% saponin (Sigma Chemical Co., St Louis, MO, USA). The cells were incubated with 100 μl staining buffer (PBS containing 0.1% bovine serum albumin and 0.01% NaN_3) containing the anti-FcγRII/III monoclonal antibody (2.4G2; rat $IgG_{2b,\kappa}$; Pharmingen, San Diego, CA, USA) to block nonspecific binding of the subsequently used antibody reagents. After 30 min, the cells were incubated for 60 min with 100 μl staining buffer containing the HMB50 antibody against human gp100 (mouse IgG; Neomarkers, Fremont, CA, USA), and then resuspended in 100 μl staining buffer containing fluorescein isothiocyanate-conjugated anti-mouse Ig_κ (187.1; Pharmingen). After incubation for 30 min, 10 000 events of the stained cells were analyzed for human gp100 protein expression by a FACSCalibur flow cytometer using CellQuest software (Becton Dickinson, Tokyo, Japan). Between all incubation steps, cells were washed three times with staining buffer.

MLR

AdRGD-gp100/mBM-DCs and Ad-gp100/mBM-DCs were prepared using corresponding vectors at an MOI of 50, and then cultured for 2 days. Three kinds of T cell, including allogenic naive T cells from intact BALB/c mouse, syngeneic naive T cells from intact C57BL/6 mouse, and syngeneic gp100-primed T cells from C57BL/6 mouse immunized intradermally with 1×10^6 AdRGD-gp100/mBM-DCs 1 week before, were purified from each mouse splenocytes as nylon wool nonadherent cells, and were used as responder cells at 1×10^5 cells/well in 96-well plates. Ad-transduced mBM-DCs, LPS/mBM-DCs, or intact mBM-DCs (stimulator cells) were inactivated by 50 μg/ml mitomycin C for 30 min and added to responder cells in varying cell numbers. Cells were cocultured in 100 μl RPMI 1640 supplemented with 10% FBS, 50 μM 2-mercaptoethanol, and antibiotics at 37°C and 5% CO_2 for 3 days. Control wells contained either stimulator cells alone or responder cells alone. Cell cultures were pulsed with 5-bromo-2′-deoxyuridine (BrdU) during the last 18 h, and then proliferation of responder cells was evaluated by Cell Proliferation ELISA, BrdU (Roche Diagnostics Co., Indianapolis, IN, USA).

Tumor protection assay

AdRGD-gp100/mBM-DCs, Ad-gp100/mBM-DCs, and AdRGD-Null/mBM-DCs were prepared using corresponding vectors at an MOI of 50. C57BL/6 mice were immunized by intradermal injection of transduced mBM-DCs into the right flank at 1×10^6 cells/50 μl. At 1 week after the vaccination, 2×10^5 B16BL6 melanoma

cells were inoculated into the mouse left flank. The size of tumors was assessed using microcalipers and was expressed as tumor volume calculated by the following formula: (tumor volume; mm^3)=(major axis; mm) × (minor axis; mm)^2 × 0.5236. Mice containing tumors >20 mm were euthanized.

Lung metastasis assay

AdRGD-gp100/mBM-DCs, Ad-gp100/mBM-DCs, and AdRGD-Null/mBM-DCs were prepared using corresponding vectors at an MOI of 1, 5, 25, or 50. For the vaccine protocol, transduced or intact mBM-DCs were intradermally injected into the flank of C57BL/6 mice at 1×10^6 cells/50 μl. At 1 week after the vaccination, 5×10^5 B16BL6 melanoma cells were injected into the tail vein. After 2 weeks lungs were excised from these mice, and then the number of metastatic nodules was counted. For the therapeutic protocol, C57BL/6 mice were intravenously injected with 5×10^5 B16BL6 cells, and immunized by intradermal injection of transduced or intact mBM-DCs into the flank at 1×10^6 cells/50 μl on days 0, 3, and 7 post-tumor injection. At 1 week after the final immunization, lungs were removed from these mice, and the number of metastatic nodules was counted.

Eu-release assay for cytolytic activity of NK cells and CTLs

AdRGD-gp100/mBM-DCs, Ad-gp100/mBM-DCs, and AdRGD-LacZ/mBM-DCs were prepared using corresponding vectors at an MOI of 50. Transduced or intact mBM-DCs were administered once intradermally into C57BL/6 mice at 1×10^6 cells/50 μl. At 1 week after immunization, nonadherent splenocytes were prepared from these mice and directly used as NK effector cells. The splenocytes were restimulated *in vitro* using B16BL6 cells, which were cultured in media containing 100 U/ml mouse IFN-γ (PeproTech EC LTD) for 24 h and inactivated with 50 μg/ml mitomycin C at 37°C for 30 min, at an effector : stimulator ratio of 10 : 1 in RPMI 1640 supplemented with 10% FBS, 50 μM 2-mercaptoethanol, and antibiotics. After five days, the splenocytes were collected and used as CTL effector cells. Target cells (IFN-γ-stimulated or untreated B16BL6, EL4 cells, and YAC-1 cells) were Eu-labeled and an Eu-release assay was performed as previously described.[55] Cytolytic activity was determined using the following formula: (% of lysis)=((experimental Eu-release−spontaneous Eu-release)/(maximum Eu-release−spontaneous Eu-release)) × 100. Spontaneous Eu-release of the target cells was <10% of maximum Eu-release by detergent in all assays.

In vivo depletion analysis

C57BL/6 mice were immunized once with 1×10^6 mBM-DCs transduced with AdRGD-gp100 at an MOI of 50, and inoculated with 1×10^5 B16BL6 cells at 1 week after immunization. At 3 days before vaccination or tumor challenge, the mice received a total of three (for vaccination) or five (for tumor challenge) intraperitoneal injections of 100 μl ascites from ICR-nu/nu mice intraperitoneally injected with GK1.5 (anti-CD4) or 53-6.72 (anti-CD8) hybridoma (kindly provided by Dr Hiroshi Yamamoto, Osaka University, Suita, Japan) or 40 μl rabbit anti-asialoGM1 antiserum (Wako Chemical Co., Osaka, Japan) at a 1 day interval. Depletion of T-cell subsets and NK cells was monitored by flow cytometry, which showed >90% specific depletion in splenocytes at the time of immunization or tumor challenge in each administration schedule.

Acknowledgements

We are grateful to Dr Hirofumi Hamada (Department of Molecular Medicine, Sapporo Medical University, Sapporo, Japan) for providing pAx1-CA h-gp100, to Dr Hiroshi Yamamoto (Department of Immunology, Graduate School of Pharmaceutical Sciences, Osaka University, Suita, Japan) for providing GK1.5 and 53-6.72 hybridoma cells, to Drs Hitoshi Kikutani and Atsushi Kumanogoh (Department of Molecular Immunology, Research Institute for Microbial Diseases, Osaka University, Suita, Japan) for technical advice about the mBM-DC preparation, and to Takashi Tsuda, Asako Matsubara, Emiko Inoue, Maki Okubo, Masaya Nishida, and Miyuki Yamanaka (Department of Biopharmaceutics, Kyoto Pharmaceutical University, Kyoto, Japan) for technical assistance.

The present study was supported in part by a Grant-in-Aid for the Encouragement of Young Scientists (13771394) from the Japan Society for the Promotion of Science; by the Research on Health Sciences focusing on Drug Innovation from The Japan Health Sciences Foundation; by grants from the Bioventure Development Program of the Ministry of Education, Culture, Sports, Science and Technology of Japan; by the Frontier Research Program of the Ministry of Education, Culture, Sports, Science and Technology of Japan; by the Science Research Promotion Fund of the Japan Private School Promotion Foundation; by Uehara Memorial Foundation; and by grants from the Ministry of Health and Welfare in Japan.

References

1 Lanzavecchia A. Identifying strategies for immune intervention. *Science* 1993; 260: 937–944.
2 Grabbe S, Beissert S, Schwarz T, Granstein RD. Dendritic cells as initiators of tumor immune responses: a possible strategy for tumor immunotherapy? *Immunol Today* 1995; 16: 117–121.
3 Steinman RM. Dendritic cells and immune-based therapies. *Exp Hematol* 1996; 24: 859–862.
4 Banchereau J, Steinman RM. Dendritic cells and the control of immunity. *Nature* 1998; 392: 245–252.
5 Fong L, Engleman EG. Dendritic cells in cancer immunotherapy. *Ann Rev Immunol* 2000; 18: 245–273.
6 Gong J, Chen D, Kashiwaba M, Kufe D. Induction of antitumor activity by immunization with fusions of dendritic and carcinoma cells. *Nat Med* 1997; 3: 558–561.
7 Yang S *et al*. Murine dendritic cells transfected with human GP100 elicit both antigen-specific CD8$^+$ and CD4$^+$ T-cell responses and are more effective than DNA vaccines at generating anti-tumor immunity. *Int J Cancer* 1999; 83: 532–540.
8 Sloan JM *et al*. MHC class I and class II presentation of tumor antigen in retrovirally and adenovirally transduced dendritic cells. *Cancer Gene Ther* 2002; 9: 946–950.
9 Herrera OB, Brett S, Lechler RI. Infection of mouse bone marrow-derived dendritic cells with recombinant adenovirus vectors leads to presentation of encoded antigen by both MHC

class I and class II molecules-potential benefits in vaccine design. *Vaccine* 2002; **21**: 231–242.
10 Wan Y *et al*. Enhanced immune response to the melanoma antigen gp100 using recombinant adenovirus-transduced dendritic cells. *Cell Immunol* 1999; **198**: 131–138.
11 Kaplan JM *et al*. Induction of antitumor immunity with dendritic cells transduced with adenovirus vector-encoding endogenous tumor-associated antigens. *J Immunol* 1999; **163**: 699–707.
12 Steitz J, Bruck J, Knop J, Tuting T. Adenovirus-transduced dendritic cells stimulate cellular immunity to melanoma via a CD4$^+$ T cell-dependent mechanism. *Gene Therapy* 2001; **8**: 1255–1263.
13 Tillman BW *et al*. T. Maturation of dendritic cells accompanies high-efficiency gene transfer by a CD 40-targeted adenoviral vector. *J Immunol* 1999; **162**: 6378–6383.
14 Asada-Mikami R *et al*. Efficient gene transduction by RGD-fiber modified recombinant adenovirus into dendritic cells. *Jpn J Cancer Res* 2001; **92**: 321–327.
15 Okada N *et al*. Efficient gene delivery into dendritic cells by fiber-mutant adenovirus vectors. *Biochem Biophys Res Commun* 2001; **282**: 173–179.
16 Okada N *et al*. Gene transduction efficiency and maturation status in mouse bone marrow-derived dendritic cells infected with conventional or RGD fiber-mutant adenovirus vectors. *Cancer Gene Ther* 2003; **10**: 421–431.
17 Dmitriev I *et al*. An adenovirus vector with genetically modified fibers demonstrates expanded tropism via utilization of a coxsackievirus and adenovirus receptor-independent cell entry mechanism. *J Virol* 1998; **72**: 9706–9713.
18 Okada N *et al*. Efficient antigen gene transduction using Arg-Gly-Asp fiber-mutant adenovirus vectors can potentiate anti-tumor vaccine efficacy and maturation of murine dendritic cells. *Cancer Res* 2001; **61**: 7913–7919.
19 Kawakami Y *et al*. Identification of a human melanoma antigen recognized by tumor-infiltrating lymphocytes associated with *in vivo* tumor rejection. *Proc Natl Acad Sci USA* 1994; **91**: 6458–6462.
20 Bloom MB *et al*. Identification of tyrosinase-related protein 2 as a tumor rejection antigen for the B16 melanoma. *J Exp Med* 1997; **185**: 453–459.
21 Coulie PG *et al*. A new gène coding for a differentiation antigen recognized by autologous cytolytic T lymphocytes on HLA-A2 melanomas. *J Exp Med* 1994; **180**: 35–42.
22 Kawakami Y *et al*. Cloning of the gene coding for a shared human melanoma antigen recognized by autologous T cells infiltrating into tumor. *Proc Natl Acad Sci USA* 1994; **91**: 3515–3519.
23 Robbins PF *et al*. Recognition of tyrosinase by tumor-infiltrating lymphocytes from a patient responding to immunotherapy. *Cancer Res* 1994; **54**: 3124–3126.
24 Rosenberg SA *et al*. Immunologic and therapeutic evaluation of a synthetic peptide vaccine for the treatment of patients with metastatic melanoma. *Nat Med* 1998; **4**: 321–327.
25 Nestle FO *et al*. Vaccination of melanoma patients with peptide-or tumor lysate-pulsed dendritic cells. *Nat Med* 1998; **4**: 328–332.
26 Perricone MA *et al*. Immunogene therapy for murine melanoma using recombinant adenoviral vectors expressing melanoma-associated antigens. *Mol Ther* 2000; **1**: 275–284.
27 Zhai Y *et al*. Cloning and characterization of the genes encoding the murine homologues of the human melanoma antigens MART1 and gp100. *J Immunother* 1997; **20**: 15–25.
28 Austyn JM. New insights into the mobilization and phagocytic activity of dendritic cells. *J Exp Med* 1996; **183**: 1287–1292.
29 Lutz MB *et al*. An advanced culture method for generating large quantities of highly pure dendritic cells from mouse bone marrow. *J Immunol Methods* 1999; **223**: 77–92.
30 Inaba K *et al*. Generation of large numbers of dendritic cells from mouse bone marrow cultures supplemented with granulocyte/macrophage colony-stimulating factor. *J Exp Med* 1992; **176**: 1693–1702.
31 Bender A *et al*. Improved methods for the generation of dendritic cells from nonproliferating progenitors in human blood. *J Immunol Methods* 1996; **196**: 121–135.
32 Reeves ME *et al*. Retroviral transduction of human dendritic cells with a tumor-associated antigen gene. *Cancer Res* 1996; **56**: 5672–5677.
33 Metharom P, Ellem KA, Schmidt C, Wei MQ. Lentiviral vector-mediated tyrosinase-related protein 2 gene transfer to dendritic cells for the therapy of melanoma. *Hum Gene Ther* 2001; **12**: 2203–2213.
34 Esslinger C, Romero P, MacDonald HR. Efficient transduction of dendritic cells and induction of a T-cell response by third-generation lentivectors. *Hum Gene Ther* 2002; **13**: 1091–1100.
35 Arthur JF *et al*. A comparison of gene transfer methods in human dendritic cells. *Cancer Gene Ther* 1997; **4**: 17–25.
36 Mackensen A *et al*. Homing of intravenously and intralymphatically injected human dendritic cells generated *in vitro* from CD34$^+$ hematopoietic progenitor cells. *Cancer Immunol Immunother* 1999; **48**: 118–122.
37 Lappin MB *et al*. Analysis of mouse dendritic cell migration *in vivo* upon subcutaneous and intravenous injection. *Immunology* 1999; **98**: 181–188.
38 Kirk CJ, Mule JJ. Gene-modified dendritic cells for use in tumor vaccines. *Hum Gene Ther* 2000; **11**: 797–806.
39 Van Tendeloo VF, Van Broeckhoven C, Berneman ZN. Gene-based cancer vaccines: an *ex vivo* approach. *Leukemia* 2001; **15**: 545–558.
40 Sarantou T *et al*. Melanoma-associated antigens as messenger RNA detection markers for melanoma. *Cancer Res* 1997; **57**: 1371–1376.
41 Zhai Y *et al*. Antigen-specific tumor vaccines. Development and characterization of recombinant adenoviruses encoding MART 1 or gp100 for cancer therapy. *J Immunol* 1996; **156**: 700–710.
42 Rea D *et al*. Highly efficient transduction of human monocyte-derived dendritic cells with subgroup B fiber-modified adenovirus vectors enhances transgene-encoded antigen presentation to cytotoxic T cells. *J Immunol* 2001; **166**: 5236–5244.
43 Prehn RT. The paradoxical association of regression with a poor prognosis in melanoma contrasted with a good prognosis in keratoacanthoma. *Cancer Res* 1996; **56**: 937–940.
44 Wildemore IV JK *et al*. Locally recurrent malignant melanoma characteristics and outcomes: a single-institution study. *Ann Plast Surg* 2001; **46**: 488–494.
45 Fernandez NC *et al*. Dendritic cells directly trigger NK cell functions: cross-talk relevant in innate anti-tumor immune responses *in vivo*. *Nat Med* 1999; **5**: 405–411.
46 Amakata Y *et al*. Mechanism of NK cell activation induced by coculture with dendritic cells derived from peripheral blood monocytes. *Clin Exp Immunol* 2001; **124**: 214–222.
47 Miller G *et al*. Adenovirus infection enhances dendritic cell immunostimulatory properties and induces natural killer and T-cell-mediated tumor protection. *Cancer Res* 2002; **62**: 5260–5266.
48 Wan Y *et al*. 'Genetically modified dendritic cells prime autoreactive T cells through a pathway independent of CD40L and interleukin 12: implications for cancer vaccines. *Cancer Res* 2000; **60**: 3247–3253.
49 Curiel-Lewandrowski C *et al*. Transfection of immature murine bone marrow-derived dendritic cells with the granulocyte–macrophage colony-stimulating factor gene potently enhances their *in vivo* antigen-presenting capacity. *J Immunol* 1999; **163**: 174–183.
50 Melero I *et al*. Intratumoral injection of bone-marrow derived dendritic cells engineered to produce interleukin-12 induces complete regression of established murine transplantable colon adenocarcinomas. *Gene Therapy* 1999; **6**: 1779–1784.
51 Kikuchi T *et al*. Dendritic cells genetically modified to express CD40 ligand and pulsed with antigen can initiate antigen-

specific humoral immunity independent of CD4+ T cells. *Nat Med* 2000; 6: 1154–1159.

52 Mizuguchi H, Kay MA. Efficient construction of a recombinant adenovirus vector by an improved *in vitro* ligation method. *Hum Gene Ther* 1998; 9: 2577–2583.

53 Mizuguchi H, Kay MA. A simple method for constructing E1- and E1/E4-deleted recombinant adenoviral vectors. *Hum Gene Ther* 1999; 10: 2013–2017.

54 Mizuguchi H *et al*. A simplified system for constructing recombinant adenoviral vectors containing heterologous peptides in the HI loop of their fiber knob. *Gene Therapy* 2001; 8: 730–735.

55 Okada N *et al*. Administration route-dependent vaccine efficiency of murine dendritic cells pulsed with antigens. *Br J Cancer* 2001; 84: 1564–1570.

Available online at www.sciencedirect.com
SCIENCE DIRECT
ELSEVIER
Biochemical Pharmacology 66 (2003) 133–140
Biochemical Pharmacology
www.elsevier.com/locate/biochempharm

The role of c-Myc on granulocyte colony-stimulating factor-dependent neutrophilic proliferation and differentiation of HL-60 cells

Toshie Kanayasu-Toyoda[a], Teruhide Yamaguchi[a,*], Tadashi Oshizawa[a], Eriko Uchida[a], Takao Hayakawa[b]

[a]*Division of Cellular and Gene Therapy Products, National Institute of Health, 1-18-1, Kamiyoga, Setagaya-Ku, 158-8501 Tokyo, Japan*
[b]*National Institute of Health Sciences, 1-18-1, Kamiyoga, Setagaya-Ku, 158-8501 Tokyo, Japan*

Received 20 August 2002; accepted 20 March 2003

Abstract

We have previously suggested that phosphatidylinositol 3-kinase (PI3K)/p70 S6 kinase (p70 S6K) plays an important role in the regulation of neutrophilic differentiation of HL-60 cells on the basis of analysis of transferrin receptor (Trf-R)-positive (Trf-R^+) and -negative (Trf-R^-) cells that appear after treatment with dimethyl sulfoxide (DMSO). In the present study, we analyzed the downstream events of p70 S6K in differentiation and proliferation of both cell types, with a particular focus on c-Myc. Similar to p70 S6K, we found that the expression of c-Myc in Trf-R^+ cells is also higher than that in Trf-R^- cells. Wortmannin, a specific inhibitor of PI3K, partially inhibited G-CSF-induced p70 S6K activity, c-Myc expression, and G-CSF-dependent proliferation, whereas rapamycin, an inhibitor of p70 S6K, completely inhibited p70 S6K activity, c-Myc expression, and G-CSF-dependent proliferation, indicating that the extent of c-Myc inhibition by these inhibitors correlates with a reduction in proliferation, and that c-Myc is downstream from PI3K/p70 S6K. We also determined phosphorylation of the 4E-binding protein 1 (4E-BP1), which is regulated downstream of the mammalian target of rapamycin. The addition of G-CSF failed to enhance the phosphorylation state of 4E-BP1 of HL-60 cells 2 days after DMSO differentiation. An antisense oligonucleotide for c-*myc* inhibited both G-CSF-dependent enhancement of c-Myc expression and proliferation in Trf-R^+ cells, but did not enhance the differentiation in terms of O_2^--generating ability or fMLP-R expression. In contrast, antisense oligonucleotide for c-*myc* promoted fMLP-R on non-treated HL-60 cells. We therefore conclude that the PI3K/p70 S6K/c-Myc cascade plays an important role in neutrophilic proliferation in HL-60 cells. Unlike that of rapamycin, however, the antisense oligonucleotide for c-*myc* could not promote differentiation of Trf-R^+ cells cultured with G-CSF, indicating that another target downstream of p70 S6K may control the differentiation of HL-60 cells in terms of the signal transduction of G-CSF.

Keywords: c-Myc; p70 S6 kinase; Phosphatidylinositol 3-kinase; Granulocyte colony-stimulating factor; HL-60 cells; Neutrophilic differentiation

1. Introduction

G-CSF plays a pivotal role in neutrophilic development. Mice deficient in either G-CSF or its receptor genes have a reduced number of neutrophils [1,2]. We have reported that G-CSF enhances the phosphorylation of p70 S6K in DMSO-treated HL-60 cells undergoing neutrophilic differentiation [3]. Furthermore, we found that during the neutrophilic differentiation of DMSO-treated HL-60 cells, Trf-R-positive (Trf-R^+) and -negative (Trf-R^-) cells appeared 2 days after the addition of DMSO, and these Trf-R^+ and Trf-R^- cells were characterized as proliferative- and differentiation-type cells, respectively [4]. We also showed that while G-CSF enhances proliferation of Trf-R^+ cells via stimulation of p70 S6K phosphorylation [4], S6K activity, and PI3K activity [5], and enhances differentiation of Trf-R^- cells via stimulation of tyrosine phosphorylation of STAT3. Rapamycin was found not only to enhance the differentiation of Trf-R^+ and Trf-R^- cells,

* Corresponding author. Tel./fax: +81-3-3700-1926.
E-mail address: yamaguch@nihs.go.jp (T. Yamaguchi).

Abbreviations: DMSO, dimethyl sulfoxide; G-CSF, granulocyte colony-stimulating factor; Trf-R, transferrin receptor; BSA, bovine serum albumin; PBS, phosphate-buffered saline; PI3K, phosphatidylinositol 3-kinase; p70 S6K, protein 70 S6 kinase; SDS–PAGE, sodium dodecyl sulfate–polyacrylamide gel electrophoresis; mTOR, mammalian target of rapamycin; 4E-BP1, 4E-binding protein 1; fMLP-R, formyl-Met-Leu-Phe receptor.

0006-2952/03/$ – see front matter
doi:10.1016/S0006-2952(03)00247-8

but to eliminate the difference in differentiation ability between Trf-R^+ and Trf-R^- cells in the presence of G-CSF. From these results, we concluded that downstream signaling components of a mTOR, which includes p70 S6K, play a negative role in the neutrophilic differentiation of HL-60 cells [4].

c-Myc is a transcription factor of the basic helix–loop–helix leucine zipper (bHLH-LZ) family that heterodimerizes with Max, another bHLH-LZ protein. The binding of Myc–Max heterodimers to E boxes (canonical consensus sequence CACGTG) activates the transcription of multiple genes implicated in the regulation of cell metabolism, protein synthesis, cell division, and apoptosis [6]. c-Myc can also repress the expression of a number of genes and decrease cell differentiation by unclear mechanisms. Constitutive c-Myc expression is observed in many human cancers, including lung carcinomas and Burkitt's lymphomas [6]. In differentiated cells, including fibroblasts, smooth muscle cells, and hepatocytes, c-Myc overexpression stimulates cell growth and proliferation, decreases cell differentiation, and sensitizes cells to apoptosis [7–10]. Treating HL-60 cells with c-*myc* antisense oligonucleotide results in the inhibition of cellular proliferation [11–13] and induces differentiation of HL-60 cells [13–15].

PI3K is reported to play an important role in the activation of p70 S6K [16–18]. From data obtained using Trf-R^+ and Trf-R^- cells, we have recently reported that, being upstream from p70 S6K, PI3K plays an important role in differentiation and proliferation [5]. Law *et al.* have reported that c-Myc is down-regulated by the inhibition of p70 S6K [19]. However, the role of c-Myc in neutrophilic differentiation and the identity of its upstream regulator, which is induced by G-CSF, remains unelucidated. In the present study, we analyzed the regulation of c-Myc expression and its role in the G-CSF-dependent signaling pathway in differentiation of neutrophilic HL-60 cells in the relationship with p70 S6K.

2. Materials and methods

2.1. Reagents

Recombinant human G-CSF was a kind gift from Chugai Pharmaceutical Co. The magnetic cell-sorting kit, MACS, was from Miltenyi Biotec. DMSO was from Pierce. The mouse anti-human Trf-R (CD 71) monoclonal antibody and the mouse anti-human c-Myc protein monoclonal antibody were purchased from Pharmingen. The rabbit anti-human 4E-BP1 polyclonal antibody was from Cell Signaling Technology Inc. The horseradish peroxidase-conjugated sheep anti-mouse IgG antibody was from Amersham Life Science Corp. Rapamycin was purchased from Calbiochem-Novabiochem Intl. Wortmannin was from Wako Pure Chemical Industries, Ltd. [γ-^{33}P]ATP was from Amersham Pharmacia Biotech.

2.2. Cell culture and differentiation in relation to neutrophilic granulocyte lineage

HL-60 cells were kindly supplied by the Japanese Cancer Research Resources Bank. Cells were maintained in RPMI 1640 medium containing 10% heat-inactivated FBS and 30 mg/L kanamycin sulfate at 37° under moisturized air containing 5% CO_2. HL-60 cells were differentiated into neutrophilic cells by the addition of DMSO. Two days after addition of the differentiating agent, Trf-R^+ and Trf-R^- cells were sorted by a magnetic cell-sorter.

2.3. Magnetic cell-sorting

Magnetic cell-sorting was performed as previously reported [4]. Trf-R^+ and Trf-R^- cells were subsequently cultured with or without 50 ng/mL G-CSF in the conditioned medium. Proliferation and O_2^--generating activity were measured 5 days after magnetic cell-sorting.

To clarify the effects of rapamycin (20 ng/mL) and wortmannin (100 nM) on differentiation of HL-60 cells, both substances were preincubated with the cells for 30 min before the addition of G-CSF.

2.4. Detection of p70 S6K enzymatic activity

The activity of p70 S6K (including p85 isoforms of S6K) was determined by ^{33}P incorporation into the S6 peptide (Upstate Biotechnology). Trf-R^+ and Trf-R^- cells were stimulated by G-CSF (50 ng/mL) for 1 hr in the presence or absence of 20 ng/mL rapamycin or 100 nM wortmannin. The reaction was terminated by the addition of an ice-cold cocktail of protease and phosphatase inhibitors [4]. After centrifugation at 1800 *g* for 3 min at 4°, the cells were suspended in 1 mL of lysis buffer [4] and then sonicated at 40 W for 20 s with a Branson Sonifier. Following further centrifugation, the collected supernatant was incubated with a rabbit anti-human p70 S6K (511–525) peptide polyclonal antibody IgG (5 mg per sample, Upstate Biotechnology) at 4° for 1 hr. The reaction mixture was next incubated with 25 mL of Protein A Sepharose 4 Fast Flow (Amersham Pharmacia Biotech) at 4° for 1 hr. The immune complexes were washed twice with lysis buffer. Protein 70 S6K enzymatic activities in each sample were determined using the p70 S6K assay kit (Upstate Biotechnology).

2.5. O_2^--generating activity and formyl-Met-Leu-Phe receptor (fMLP-R) expression

The O_2^--generating activity of the differentiated cells was measured in terms of the ferricytochrome *c* reduction assay, as previously described [4]. For the fMLP-R expression assay, the differentiated cells were collected and incubated with FITC-fMLP, then were subjected to flow cytometric analysis (FACSCalibur, Becton and Dickinson).

2.6. Preparation of cell lysates and immunoblotting

For immunoblotting with anti-cMyc antibody, Trf-R^+ and Trf-R^- cells resuspended in conditioned medium were stimulated with G-CSF (50 ng/mL). After the incubation with G-CSF for 7 hr, the cells were mixed with an equal volume of ice-cold buffer containing a cocktail of protease and phosphatase inhibitors. For immunoblotting with anti-p70/p85 S6K and 4E-BP1 antibodies, HL-60 cells treated with DMSO for 2 days were stimulated by G-CSF for 30 min. The reactions were terminated by addition of the ice-cold buffer. Western blotting analysis was then performed, as described previously [4]. The bands that appeared on X-ray films were scanned and the density of each band was calculated using the public domain NIH Image program (developed at the U.S. National Institutes of Health and available on the Internet) within the linear range for quantitation.

2.7. Treatment of c-myc antisense or sense oligonucleotides

The sequences of the antisense- and sense-c-*myc* S-oligonucleotides were 5′-AACGTTGAGGGGCAT-3′ and 5′-TTGCAACTCCCCGTA-3′, respectively. These sequences were originally reported by Heikkila *et al.* [20]. The antisense- and sense-c-*myc* S-oligonucleotides were dissolved in water at 1 mM. After cell-sorting, both cells were incubated with 10 mM antisense or 10 mM sense c-*myc* oligonucleotides for 30 min. After the addition of 50 ng/mL G-CSF for 3 hr, 10 mM of each oligonucleotide was again added. Cells were subsequently cultured for 5 days, and then, both proliferation and O_2^- production were determined. Expression of fMLP-R was analyzed 3 days after the addition of antisense oligonucleotides for c-*myc*. Seven hours after the addition of G-CSF, the cells were collected and subjected to the Western blotting analysis for c-Myc expression.

2.8. Statistical analysis

Each experiment was repeated three or more times, and representative data are indicated. Statistical analysis was performed using the unpaired *t*-test. Values of $P < 0.05$ were considered to indicate statistical significance.

3. Results

3.1. Effects of wortmannin and rapamycin on proliferation of Trf-R^+ and Trf-R^- cells

To clarify the cascade of signal transduction in the proliferation of neutrophilic proliferation, we examined the effects of rapamycin, a specific inhibitor of p70 S6K, and wortmannin, a specific inhibitor of PI3K on the growth

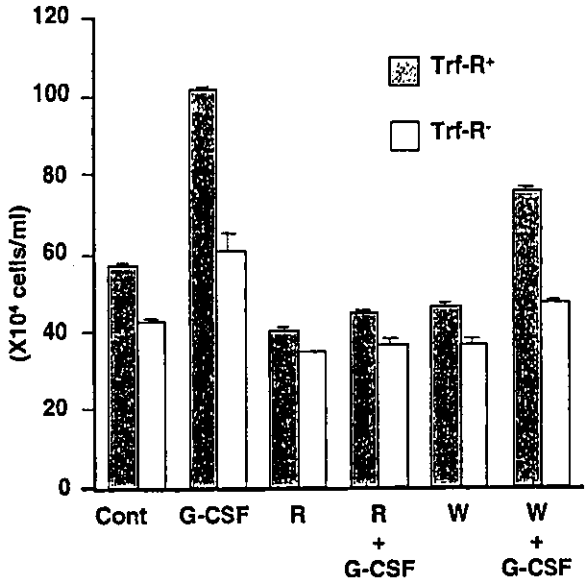

Fig. 1. Effects of rapamycin and wortmannin on G-CSF-induced proliferation in differentiating HL-60 cells. Effects of rapamycin or wortmannin on the proliferation of differentiated HL-60 cells were determined. Trf-R^+ cells and Trf-R^- cells sorted from differentiating HL-60 cells were preincubated with or without 20 ng/mL rapamycin (R) or 100 nM wortmannin (W), and then subsequently cultured with G-CSF. After a 5-day culture with G-CSF, the cell numbers in each sample were counted. Open columns denote Trf-R^- cells and gray columns Trf-R^+ cells. Columns and bars represent the mean ± SD of triplicate wells.

of Trf-R^+ and Trf-R^- cells. We have previously reported that Trf-R^+ cells and Trf-R^- cells are proliferative-type and differentiation-type cells, respectively, and that each character is enhanced by G-CSF. As shown in Fig. 1, the growth rate of Trf-R^+ cells was greater than that of Trf-R^- cells, and G-CSF markedly enhanced the proliferation of Trf-R^+ cells. Rapamycin completely inhibited G-CSF-induced proliferation of Trf-R^+ cells, as reported previously [4]. In contrast, 100 nM wortmannin completely inhibited PI3K, but only partially inhibited p70 S6K [5]; in addition, the same concentration of wortmannin only partially inhibited G-CSF-dependent proliferation of Trf-R^+ cells (Fig. 1), suggesting that PI3K partially contributes to the G-CSF-dependent proliferation of HL-60 cells.

3.2. Activity of p70 S6K in Trf-R^+ and Trf-R^- cells and the effects of wortmannin or rapamycin on p70 S6K activity and 4E-BP1 phosphorylation

To clarify the role of p70 S6K (including p85 isoforms of S6K) in the proliferation of differentiating HL-60 cells, we examined the activities of p70 S6K in Trf-R^+ and Trf-R^- cells. As shown in Fig. 2A, the p70 S6K activity of Trf-R^+ cells was higher than that in Trf-R^- cells. In the presence of G-CSF, the p70 S6K activity of Trf-R^+ cells was 2.7 times higher than that of Trf-R^- cells. In contrast, G-CSF activated ERK in neither Trf-R^+ nor Trf-R^- cells [5]. These data confirm the hypothesis that p70 S6K plays an important role in the G-CSF-dependent and -independent proliferation of neutrophils [4,5].